

ARTICLE

# CHMP2B regulates TDP-43 phosphorylation and cytotoxicity independent of autophagy via CK1

Xue Deng<sup>1,2\*</sup>, Xing Sun<sup>1,2\*</sup> , Wenkai Yue<sup>1,2\*</sup>, Yongjia Duan<sup>1</sup>, Rirong Hu<sup>1,2</sup>, Kai Zhang<sup>1,2</sup>, Jiangxia Ni<sup>1,2</sup>, Jihong Cui<sup>1</sup>, Qiangqiang Wang<sup>1</sup>, Yelin Chen<sup>1,2</sup>, Ang Li<sup>3,4,5,6</sup> , and Yanshan Fang<sup>1,2</sup> 

The ESCRT protein CHMP2B and the RNA-binding protein TDP-43 are both associated with ALS and FTD. The pathogenicity of CHMP2B has mainly been considered a consequence of autophagy–endolysosomal dysfunction, whereas protein inclusions containing phosphorylated TDP-43 are a pathological hallmark of ALS and FTD. Intriguingly, TDP-43 pathology has not been associated with the FTD-causing *CHMP2B*<sup>Intron5</sup> mutation. In this study, we identify *CHMP2B* as a modifier of TDP-43–mediated neurodegeneration in a *Drosophila* screen. Down-regulation of *CHMP2B* reduces TDP-43 phosphorylation and toxicity in flies and mammalian cells. Surprisingly, although *CHMP2B*<sup>Intron5</sup> causes dramatic autophagy dysfunction, disturbance of autophagy does not alter TDP-43 phosphorylation levels. Instead, we find that inhibition of CK1, but not TTBK1/2 (all of which are kinases phosphorylating TDP-43), abolishes the modifying effect of CHMP2B on TDP-43 phosphorylation. Finally, we uncover that CHMP2B modulates CK1 protein levels by negatively regulating ubiquitination and the proteasome-mediated turnover of CK1. Together, our findings propose an autophagy-independent role and mechanism of CHMP2B in regulating CK1 abundance and TDP-43 phosphorylation.

## Introduction

TAR DNA-binding protein 43 (TDP-43) is a DNA/RNA-binding protein participating in the assembly of various ribonucleoprotein complexes and plays an important role in regulating RNA processing and functions (Chen-Plotkin et al., 2010; Cohen et al., 2011; Lee et al., 2011). TDP-43 is also a major pathological protein linked to a spectrum of human neurodegenerative diseases, collectively known as TDP-43 proteinopathies (Arai et al., 2009; Chang et al., 2016; Hasegawa et al., 2008; Higashi et al., 2007; Neumann et al., 2009; Neumann et al., 2007; Toyoshima and Takahashi, 2014). In particular, abnormal TDP-43 protein inclusions are found in ~97% of amyotrophic lateral sclerosis (ALS) and ~45% frontotemporal dementia (FTD) patients (Ling et al., 2013; Tan et al., 2017). In many of these cases, the TDP-43 pathology is characterized by phosphorylation of the protein at serine 409 and 410 (pS409/410; Hasegawa et al., 2008; Neumann et al., 2009), and phosphorylated TDP-43 (pTDP-43) is associated with increased insolubility and cytoplasmic aggregation (Choksi et al., 2014; Hasegawa et al., 2008; Liachko et al.,

2010; Neumann et al., 2009; Nonaka et al., 2016; Yamashita et al., 2016; Zhang et al., 2010).

Casein kinase 1 (CK1) was previously shown to phosphorylate TDP-43 in vitro and in vivo (Hasegawa et al., 2008; Kametani et al., 2009; Nonaka et al., 2016). CK1 is a family of serine/threonine-selective kinases that phosphorylate key proteins in various physiological and pathological processes such as development, metabolism, cancer, and neurodegenerative disorders (Cheong and Virshup, 2011; Cozza and Pinna, 2016; Cruciat, 2014; Jiang, 2017; Perez et al., 2012). In addition, CK1 inhibitors were shown to reduce TDP-43 phosphorylation and toxicity in a variety of models, including immortalized mammalian cell lines, fly and mouse neurons, and human cells derived from ALS and FTD patients (Salado et al., 2014; Alquezar et al., 2016; Martínez-González et al., 2020). Thus, manipulation of CK1 activity has been proposed as a potential drug target for treating ALS and FTD. However, whether and how CK1 is involved in the pathogenic pathways remain unclear.

<sup>1</sup>Interdisciplinary Research Center on Biology and Chemistry, Shanghai Institute of Organic Chemistry, Chinese Academy of Sciences, Shanghai, China; <sup>2</sup>University of Chinese Academy of Sciences, Beijing, China; <sup>3</sup>Guangdong Key Laboratory of Non-human Primate Research, Guangdong-Hong Kong-Macau Institute of CNS Regeneration, Jinan University, Guangzhou, China; <sup>4</sup>Bioland Laboratory (Guangzhou Regenerative Medicine and Health Guangdong Laboratory), Guangzhou, China; <sup>5</sup>Key Laboratory of CNS Regeneration (Jinan University), Ministry of Education, Guangzhou, China; <sup>6</sup>Department of Neurology, Guangdong Neuroscience Institute, Guangdong Provincial People's Hospital, Guangdong Academy of Medical Sciences, Guangzhou, China.

\*X. Deng, X. Sun, and W. Yue contributed equally to this paper; Correspondence to Yanshan Fang: [fangys@sioc.ac.cn](mailto:fangys@sioc.ac.cn); Ang Li: [anglijnu@jnu.edu.cn](mailto:anglijnu@jnu.edu.cn).

© 2021 Deng et al. This article is distributed under the terms of an Attribution–Noncommercial–Share Alike–No Mirror Sites license for the first six months after the publication date (see <http://www.rupress.org/terms/>). After six months it is available under a Creative Commons License (Attribution–Noncommercial–Share Alike 4.0 International license, as described at <https://creativecommons.org/licenses/by-nc-sa/4.0/>).

Charged multivesicular body protein 2B (*CHMP2B*) is another gene associated with both ALS and FTD (Cox et al., 2010; Parkinson et al., 2006; Skibinski et al., 2005). It encodes the endosomal sorting complex required for transport (ESCRT) III subunit protein CHMP2B, which plays a vital role in endolysosomal trafficking, vesicle fusion, and autophagic degradation (Henne et al., 2011; Urwin et al., 2009). Among the disease-causing mutations in *CHMP2B*, the most studied is *CHMP2B<sup>Intron5</sup>* in FTD linked to chromosome 3 (FTD-3). It is a single-nucleotide (G→C) mutation in exon 6, which causes aberrant splicing inclusive of the 201 bp of intron 5 that contains a stop codon and leads to a truncation of 36 amino acids from the acidic C terminus of CHMP2B. Consequently, *CHMP2B<sup>Intron5</sup>* lacks the important binding site for Vps4, and its self-binding to the basic N terminus is significantly reduced, which disrupts the normal auto-inhibition in CHMP2B (Isaacs et al., 2011; Krasniak and Ahmad, 2016; Urwin et al., 2009). As deficits in CHMP2B and the ESCRT complex often lead to accumulation of endosomes and autophagosomes (Clayton et al., 2015; Ghazi-Noori et al., 2012; Lee et al., 2007; Urwin et al., 2010; van der Zee et al., 2008), the pathogenicity of *CHMP2B* has been considered mainly a consequence of disruption of the autophagy-endolysosomal pathway. Intriguingly, *CHMP2B<sup>Intron5</sup>* has not been associated with TDP-43 pathology in FTD-3 patients (Holm et al., 2007), whereas TDP-43 inclusion bodies are detected in the spinal motor neurons and glia of ALS patients carrying other *CHMP2B* mutations such as *CHMP2B<sup>Q206H</sup>* (Cox et al., 2010). In addition, manipulation of the ESCRT subunits other than CHMP2B caused TDP-43 aggregation (Filimonenko et al., 2007). Thus, it remains elusive whether CHMP2B and TDP-43 are molecularly linked in ALS and FTD.

In this study, we identify *CHMP2B* as a modifier of TDP-43 neurotoxicity in a fly genetic screen and reveal a previously unknown function of *CHMP2B* in regulating TDP-43 phosphorylation. This function is independent of the role of CHMP2B in autophagy, as disruption of the autophagy pathway does not alter pTDP-43 levels. Instead, we show that CHMP2B regulates the abundance of CK1 via the ubiquitin-proteasome system (UPS)-dependent protein turnover, which underlies the mitigating effect of knockdown (KD) of *CHMP2B* on TDP-43 phosphorylation and toxicity.

## Results

### Down-regulation of *CHMP2B* alleviates TDP-43 neurotoxicity and reduces TDP-43 phosphorylation levels in a *Drosophila* model

To identify unknown players involved in TDP-43-mediated neurodegeneration, we conducted a genetic screen for new modifiers of TDP-43 neurotoxicity using a *Drosophila* model that expressed human TDP-43 (*hTDP-43*) with the binary Gal4-UAS system. Transgenic expression of *hTDP-43* in the fly eyes (by a GMR-Gal4 driver) caused age-dependent degeneration, as evidenced by rough surface, loss of pigment cells, and swelling of the compound fly eyes (Fig. 1, a–d; and Fig. S1, a and b).

In the screen, we tested ~940 transgenic RNAi fly lines targeting genes involved in the regulation of proteostasis, including

autophagy and UPS, posttranslational modifications such as ubiquitination and phosphorylation, mitochondria, and others. We isolated 32 enhancer genes and 10 suppressor genes whose loss of function (LOF) modified TDP-43-mediated neurodegeneration. Among them, two fly lines (#28531 and #38375) showed remarkable suppression of hTDP-43-induced eye degeneration (Fig. 1, e and f; and Fig. S1, c and d), which turned out to be two independent RNAi lines of the fly gene *CHMP2B*. Further examination revealed that down-regulation of *CHMP2B* with an inducible pan-neuronal *elav*-GeneSwitch (*elavGS*) driver markedly mitigated hTDP-43-induced, age-dependent climbing deficits (Figs. 1 g and S1 e). Moreover, expression of *hTDP-43* in the adult fly neurons shortened the lifespan by ~20.7%, which was increased by ~14.4% with KD of *CHMP2B* (#28531) compared with transgenic expression of the control RNAi-*luciferase* transgene in the TDP-43 flies (Fig. 1 h). The other RNAi-*CHMP2B* line (#38375) also extended the lifespan of the TDP-43 flies, although to a lesser extent (Fig. S1 f). In addition, we confirmed that KD of *CHMP2B* in a WT background did not increase the climbing capability (Fig. S1, g and h) or extend the lifespan (Fig. S1, i and j), indicating that down-regulation of *CHMP2B* did not have a general beneficial effect on promoting motility or survival. Rather, it specifically suppressed TDP-43-mediated neurotoxicity in flies.

TDP-43 is known to play a vital role in regulating RNA metabolism and homeostasis (Cohen et al., 2011; Lee et al., 2011). It was reasonable to hypothesize that KD of *CHMP2B* rescued the TDP-43 flies, because *CHMP2B* was abnormally up-regulated by overexpression (OE) of *hTDP-43*. We hence examined the mRNA levels of *CHMP2B* by real-time quantitative PCR (qPCR) analysis; however, it showed no significant change of the *CHMP2B* mRNA levels in the TDP-43 fly heads (Fig. 1 i). Considering the known function of CHMP2B and ESCRT in the autophagy-endolysosomal pathway and proteostasis, the alternative possibility was that KD of *CHMP2B* might affect TDP-43 abundance. We then examined TDP-43 protein levels in the RNAi-*CHMP2B* flies by Western blotting. Interestingly, although the total TDP-43 abundance was unchanged, we found the disease hallmarked pS409/410 phosphorylation of TDP-43 (Hasegawa et al., 2008; Neumann et al., 2009) was reduced by RNAi-*CHMP2B* (Fig. 1, j–l). Transgenic OE of the FTD-3 associated mutation *CHMP2B<sup>Intron5</sup>* in flies caused the fly eye to degenerate (Fig. S2 a; Ahmad et al., 2009), and we showed that OE of *CHMP2B<sup>Intron5</sup>* increased the phosphorylation levels of hTDP-43 in fly neurons (Fig. S2, b–d). Neither KD of *CHMP2B* nor OE of *CHMP2B<sup>Intron5</sup>* significantly affected the insolubility of hTDP-43 (Fig. S2, e–h), indicating that the transgenically overexpressed soluble hTDP-43 protein manifested significant toxicity in the fly model.

### *CHMP2B* abundance regulates TDP-43 phosphorylation and toxicity in mammalian cells

Next, we extended our study to mammalian systems to see whether the function of *CHMP2B* in regulating TDP-43 phosphorylation and toxicity was evolutionarily conserved. Consistent with the observations in flies, KD of *CHMP2B* in human 293T cells also decreased pTDP-43 levels (Fig. 2, a–c). Of note, since little endogenous TDP-43 was phosphorylated in 293T cells

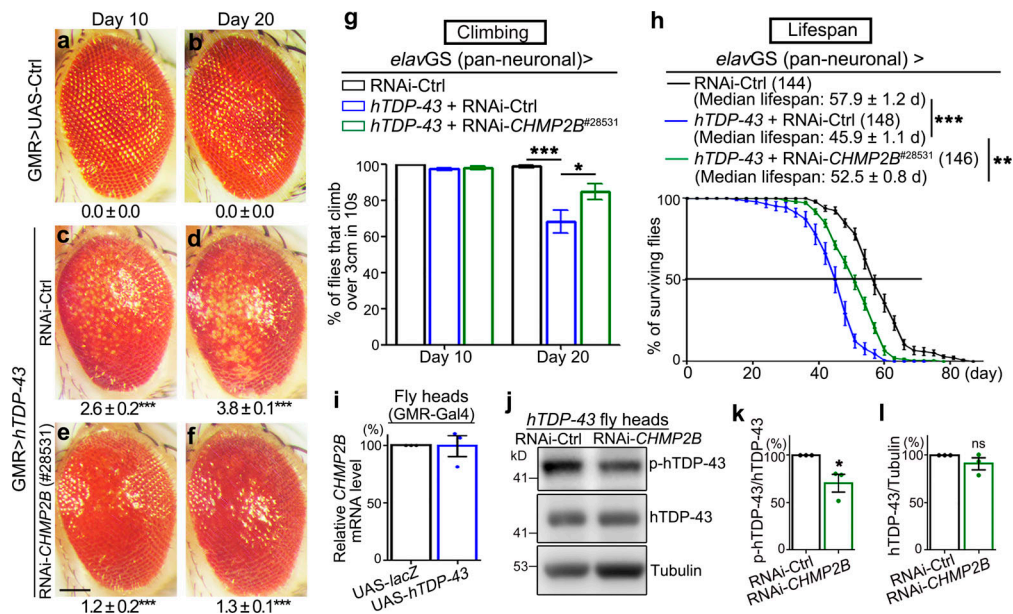


**Figure 1. CHMP2B modifies the neurotoxicity and affects the phosphorylation levels of hTDP-43 in an in vivo *Drosophila* model.** (a–f) KD of *CHMP2B* (#28531; *GMR-Gal4*) suppresses hTDP-43-induced eye degeneration in flies. The degeneration score (mean ± SEM) and the statistical significance compared with the *UAS-lacZ* (*UAS-Ctrl*) flies are indicated. (g and h) Adult-onset, neuronal (*elavGS*) down-regulation of *CHMP2B* suppresses hTDP-43-induced climbing deficits (g) and extends the shortened lifespan (h). RNAi-Ctrl, RNAi-*luciferase* flies. (i) qPCR analysis of the mRNA levels of *CHMP2B* in the heads of TDP-43 flies. The mRNA levels are normalized to *actin* and shown as the average percentage compared to that of the control flies (*UAS-lacZ*). (j–l) Western blot analysis (j) and quantifications of phosphorylation (p409/410; k) and total protein levels (l) of hTDP-43 in the fly heads. hTDP-43, human TDP-43; p-hTDP-43, phosphorylated hTDP-43. The protein levels are normalized to tubulin or total hTDP-43 and shown as percentages to that of the RNAi-Ctrl group. Mean ± SEM,  $n = \sim 10$  eyes/group (a–f),  $n = \sim 10$  vials/group with  $\sim 20$  flies per vial (g); the number of flies tested in each group is as indicated (h); and  $n = 3$  (i, k, and l). Statistical significance is determined by one-way ANOVA with Tukey’s HSD post-hoc test (a–f, g), two-tailed Student’s *t* test in (i, k, and l) and two-way ANOVA with Bonferroni’s post-hoc test in (h) at \*,  $P < 0.05$ ; \*\*,  $P < 0.01$ ; \*\*\*,  $P < 0.001$ . ns, not significant. Scale bar, 100  $\mu$ m. Source data are available for this figure: SourceData F1.

under normal conditions (lane 1 in Fig. 2 d), TDP-43 was overexpressed by transient transfection of TDP-43-HA in this experiment. This was to increase the basal TDP-43 phosphorylation levels in order to examine whether RNAi-*CHMP2B* could reduce pTDP-43 levels. Importantly, we showed that up-regulation of WT *CHMP2B* dramatically increased the phosphorylation levels of endogenous TDP-43 in 293T cells (Fig. 2, d and e) without affecting the TDP-43 protein abundance (Fig. 2, d and f). OE of *CHMP2B<sup>Intron5</sup>* in 293T cells also increased the pTDP-43 levels compared with the vector control, but to a lesser extent compared with that by OE of WT *CHMP2B* (Fig. 2, d–f).

We went on to determine how manipulation of *CHMP2B* affected TDP-43 toxicity using a Cell Counting Kit 8 (CCK8) assay. OE of TDP-43 in 293T cells reduced the cell viability, which was suppressed by KD of *CHMP2B* (Fig. 2 g) and enhanced by OE of WT *CHMP2B* (Fig. 2 h). OE of *CHMP2B<sup>Intron5</sup>* enhanced TDP-43-induced loss of cell viability even more (Fig. 2 h), although it only mildly increased TDP-43 phosphorylation compared with OE of WT *CHMP2B* (Fig. 2, d–f), suggesting alternative mechanisms conferring to the cytotoxicity of *CHMP2B<sup>Intron5</sup>*.

Since *CHMP2B* and the ESCRT complex play an important role in the autophagy–endolysosomal pathway and proteostasis regulation, we examined how manipulation of *CHMP2B* impacted on the solubility of TDP-43. Again, since endogenous TDP-43 was predominantly soluble in 293T cells, the effect on TDP-43 solubility was assessed with the transiently

overexpressed TDP-43-HA in the subsequent experiments. We found that KD of *CHMP2B* reduced (Fig. 2, i and j), whereas OE of WT *CHMP2B* or *CHMP2B<sup>Intron5</sup>* increased (Fig. 2, k and l), the insolubility of TDP-43-HA in 293T cells. Of note, unlike the mild effect in promoting TDP-43 phosphorylation (Fig. 2, d–f), OE of *CHMP2B<sup>Intron5</sup>* increased the insolubility of TDP-43 to the similar or slightly higher level than that of OE of WT *CHMP2B* (Fig. 2, k and l).

### The autophagy pathway does not profoundly impact on TDP-43 phosphorylation

Previous studies of *CHMP2B<sup>Intron5</sup>* revealed remarkable autophagy dysfunction (Krasniak and Ahmad, 2016; Lee et al., 2007; Lee et al., 2009) and inhibition of autophagy could suppress the toxicity of *CHMP2B<sup>Intron5</sup>* in cultured cortical neurons (Lee and Gao, 2009). Indeed, we found that in the fly heads overexpressing *CHMP2B<sup>Intron5</sup>*, the protein levels of lipidated autophagy-related 8a (ATG8A-II, the *Drosophila* homologue of the mammalian LC3-II; Kabeya et al., 2000) and refractory to sigma P (Ref(2)P, P62 in mammals; Bjørkøy et al., 2005) were dramatically increased (Fig. 3, a–c). Inhibition of autophagy induction by KD of *Atg12* or *Atg17* significantly suppressed TDP-43-induced eye degeneration in flies (Fig. 3, d and e). However, the phosphorylation levels of hTDP-43 in the RNAi-*Atg12* or RNAi-*Atg17* flies were unaffected (Fig. 3, f–h), suggesting that the autophagy pathway did not play a major role in regulating TDP-43 phosphorylation in the fly model.

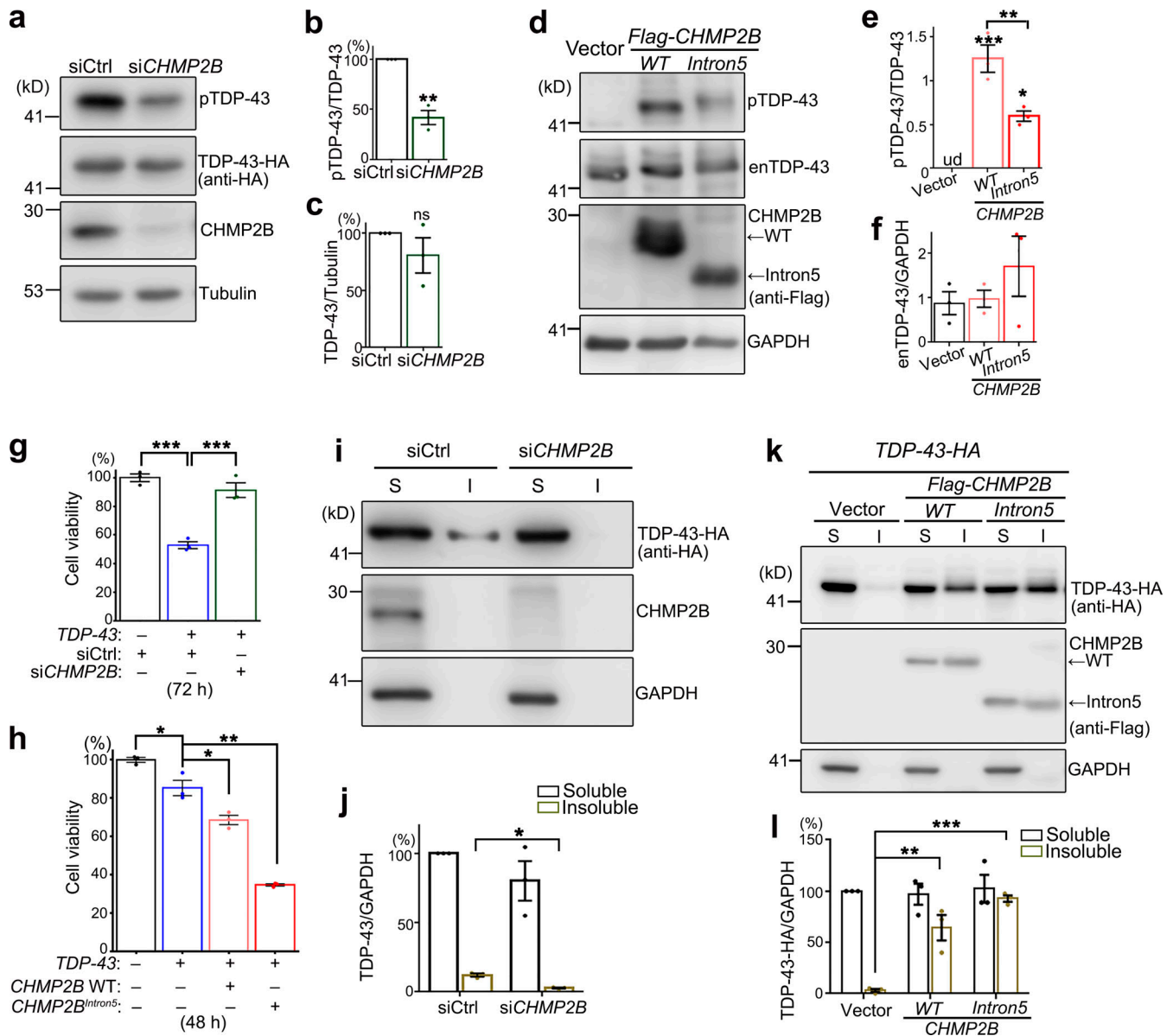


**Figure 2. CHMP2B regulates TDP-43 phosphorylation and toxicity in 293T cells.** (a–c) Representative Western blotting images (a) and quantifications (b and c) of TDP-43-HA phosphorylation (b) and protein levels (c) in 293T cells treated with the siRNA of *CHMP2B* (siCHMP2B). (d–f) OE of WT *CHMP2B* or *CHMP2B<sup>Intron5</sup>* increases the phosphorylation levels of endogenous TDP-43 (enTDP-43) in 293T cells. ud, undetected. (g and h) KD of *CHMP2B* suppresses (g), whereas OE of WT *CHMP2B* or *CHMP2B<sup>Intron5</sup>* enhances (h), TDP-43-induced loss of cell viability. siCtrl, scrambled siRNA. Cells are homogenized and examined using a CCK8 assay at 72 h after transfection of siRNA and the TDP-43-HA expression plasmid (g) or at 48 h after transfection of the expression plasmids only (h). (i–l) Representative Western blot images (i and k) and quantification (j and l) of TDP-43-HA proteins in the soluble (S, supernatants in RIPA) and insoluble (I, pellets resuspended in 9 M urea) fractions of the cell lysates of 293T cells treated with siCHMP2B (i and j) or transfected with WT *CHMP2B* or *CHMP2B<sup>Intron5</sup>* (k and l). siCtrl, scrambled siRNA. All protein levels are normalized to GAPDH in the soluble fraction. Mean ± SEM; n = 3. Two-tailed Student's t test in (b, c, and j) and one-way ANOVA with Tukey's HSD post-hoc test (e–h and l); \*, P < 0.05; \*\*, P < 0.01; \*\*\*, P < 0.001. ns, not significant. Source data are available for this figure: SourceData F2.

In mammalian cell cultures, we found that KD of *CHMP2B* increased the levels of the autophagy marker LC3-II, while OE of WT *CHMP2B* increased both LC3-II and P62 (Fig. 3, i–n). Both down- and up-regulation of *CHMP2B* impaired autophagic flux, indicating that a steady level of *CHMP2B* was critical for maintaining normal autophagy function. This was in contrast to the dose-dependent effect of *CHMP2B* on pTDP-43 levels (Fig. 2, a–f). OE of *CHMP2B<sup>Intron5</sup>* caused a more severe autophagic

dysfunction, as a strikingly more accumulation of LC3-II was detected even when *CHMP2B<sup>Intron5</sup>* was expressed at a lower level than WT *CHMP2B* (Fig. 3, l–n), which suggested that the *CHMP2B<sup>Intron5</sup>* mutation was likely a hypermorphic or dominant allele for the function in regulating autophagy.

Nevertheless, induction of autophagy by treating the cells with rapamycin (Rapa; Fig. 3, o and p; which mimicked the effect of siCHMP2B on autophagy in Fig. 3, i–k) or disruption of the

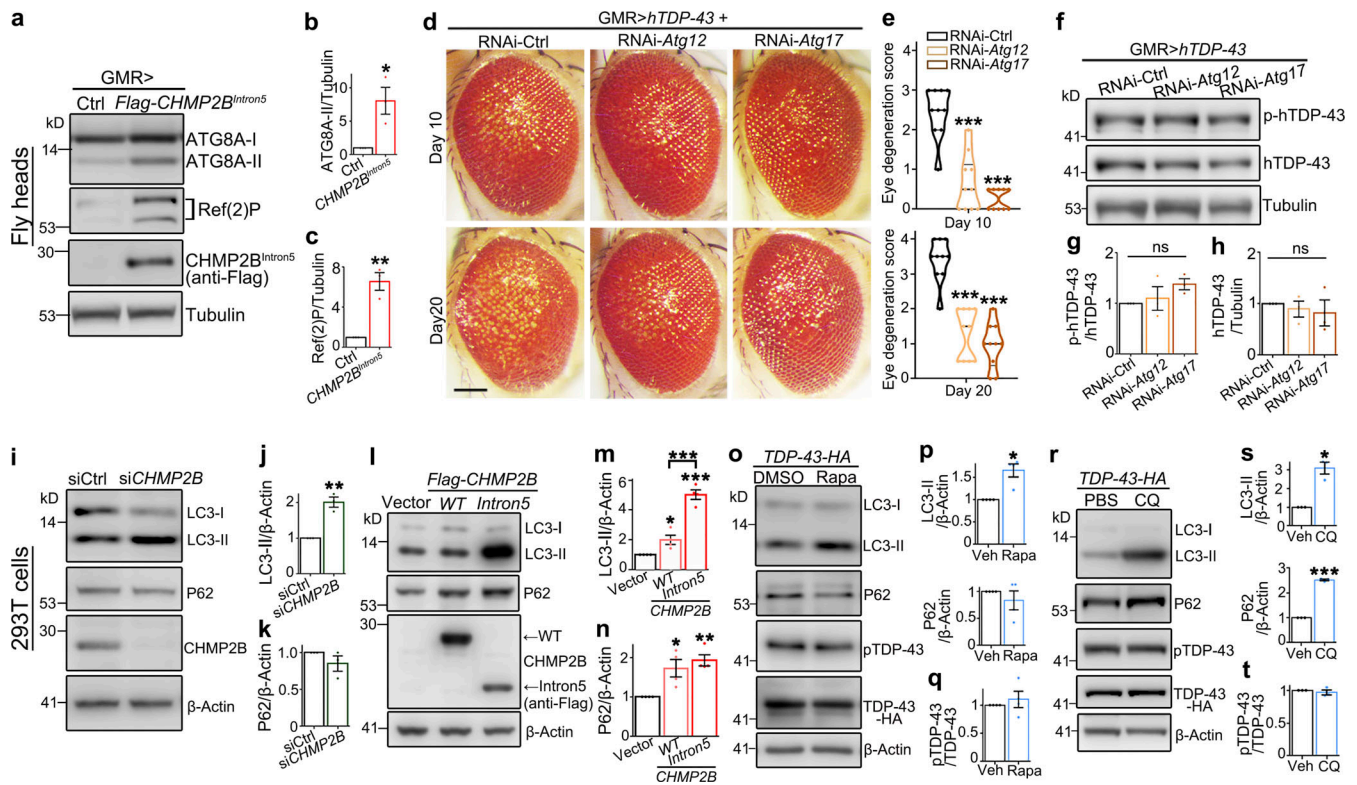


**Figure 3. Disturbance of the autophagy-lysosomal pathway does not alter TDP-43 phosphorylation levels in flies or mammalian cells.** (a–c) Western blot analysis (a) shows the levels of ATG8A-II (b) and Ref(2)P (c) are significantly increased in the fly heads transgenically expressing human *CHMP2B<sup>Intron5</sup>* (*GMR>Gal4*). Ctrl, *UAS-luciferase*. (d and e) Inhibition of autophagy by RNAi-*Atg12* or RNAi-*Atg17* attenuates hTDP-43-induced eye degeneration in flies (d), quantified with violin plots (e). RNAi-Ctrl, RNAi-*mCherry*. (f–h) Western blot analysis (f) shows unaffected phosphorylation (g) and total protein (h) levels of TDP-43 in the RNAi-*Atg12* and RNAi-*Atg17* fly heads. hTDP-43, human TDP-43; p-hTDP-43, phosphorylated hTDP-43. (i–n) Western blot analyses (i and l) and quantifications (j, k, m, and n) of LC3-II and P62 levels in 293T cells treated with si*CHMP2B* (i–k) or OE of *CHMP2B* or *CHMP2B<sup>Intron5</sup>* (l–n). siCtrl, scrambled siRNA. (o–t) Western blot analyses of LC3-II, P62, and pTDP-43 levels in 293T cells treated with Rapa (100 nM, 1 h; o–q) or CQ (10 μM, 12 h; r–t). Vehicle controls: DMSO for Rapa and PBS for CQ. Mean ± SEM, *n* = 3–4 in all Western blots and *n* = 10 flies/group (e). Two-tailed Student's *t* test (b, c, j, k, p, q, s, and t) and one-way ANOVA with Tukey's HSD post-hoc test (e, g, h, m, and n); \*, *P* < 0.05; \*\*, *P* < 0.01; \*\*\*, *P* < 0.001. ns, not significant. Scale bar, 100 μm. Source data are available for this figure: SourceData F3.

autophagic flux with chloroquine (CQ; Fig. 3, r–s, which mimicked the effect of OE of WT *CHMP2B* and *CHMP2B<sup>Intron5</sup>* on autophagy in Fig. 3, l–n) did not significantly alter pTDP-43 levels (Fig. 3, o, q, r, and t). Likewise, genetic inhibition of autophagy by siRNA-mediated KD of *Atg12* or *Atg17* also attenuated TDP-43-induced loss of cell viability in 293T cells (Fig. S3 a). KD of *Atg12* or *Atg17* decreased the level of the autophagy marker LC3-II and increased that of P62 (Fig. S3, b–d), indicating that autophagy was indeed disturbed. Nevertheless, pTDP-43 levels were unchanged by KD of *Atg12* or *Atg17* (Fig. S3, b and e). Together, both the in vivo observations in flies and the pharmacological and genetic manipulations in mammalian cell cultures indicate that autophagy does not play a major role in regulating pTDP-43 levels and that the modifying effect of *CHMP2B* on TDP-43 phosphorylation is independent of the autophagy pathway.

### CHMP2B promotes TDP-43 hyperphosphorylation and cytotoxicity via CK1

Seeking for an alternative mechanism to explain how *CHMP2B* regulated TDP-43 phosphorylation, we looked through literature

and found the protein kinase CK1 was previously reported to phosphorylate TDP-43 (Hasegawa et al., 2008; Kametani et al., 2009). Consistently, we found that increase of CK1 activity by OE of *CK1α* or *CK1δ* in 293T cells promoted phosphorylation of the endogenous TDP-43 protein in 293T cells (Fig. 4, a and b). Further, KD of *CK1α* or *CK1δ* decreased the phosphorylation levels of transiently overexpressed TDP-43-HA (Fig. 4, c and d). More importantly, KD of *CK1α* and *CK1δ* significantly suppressed *CHMP2B* OE-induced hyperphosphorylation of endogenous TDP-43 (Fig. 4, e and f).

Consistent with their effects on TDP-43 phosphorylation, we found that down-regulation of *CK1α* or *CK1δ* ameliorated the cytotoxicity caused by OE of TDP-43 (Fig. 4 g) or *CHMP2B* (Fig. 4 h), whereas up-regulation of *CK1α* or *CK1δ* diminished the mitigating effect of si*CHMP2B* on TDP-43-mediated cytotoxicity (Fig. 4 i). Of note, because of the critical role of CK1 in various other cellular functions and cell survival (Cheong and Virshup, 2011; Cruciat, 2014; Jiang, 2017), the amounts of transfected siRNAs (0.8 nM of si*CK1α* and 0.16 nM of si*CK1δ*) and the expression plasmids (10 ng of *CK1α* and 5 ng of *CK1δ*) were carefully determined so that OE or KD of CK1 per se did not manifest significant toxicity in these cell viability assays (Fig. S4, a and b).

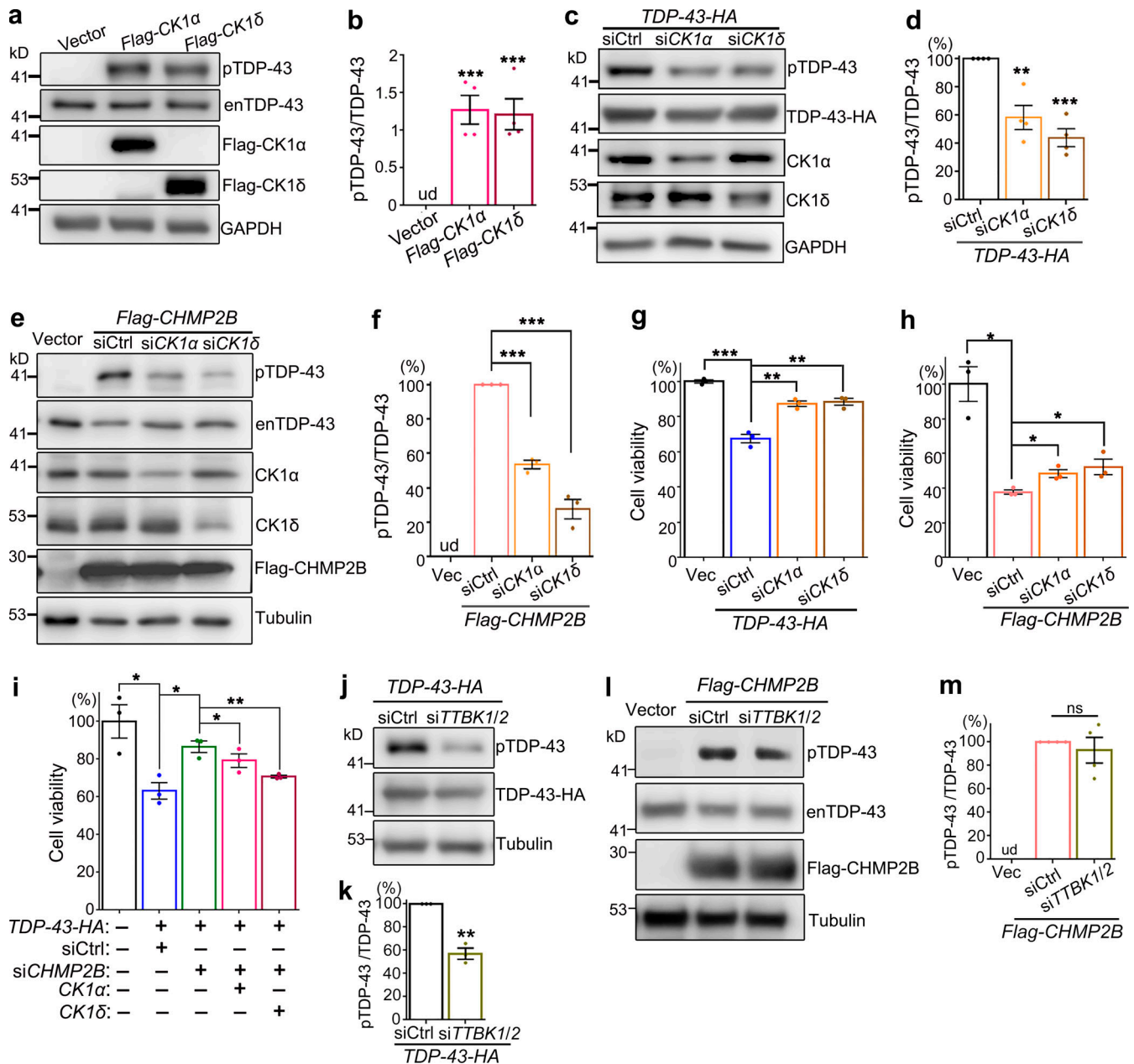


**Figure 4. The kinase CK1 mediates the modifying effects of CHMP2B on TDP-43 phosphorylation and cytotoxicity. (a–d)** OE of CK1 $\alpha$  or CK1 $\delta$  promotes hyperphosphorylation of endogenous TDP-43 (enTDP-43; a and b), whereas KD of CK1 $\alpha$  or CK1 $\delta$  reduces pTDP-43-HA levels in 293T cells (c and d). **(e and f)** KD of CK1 $\alpha$  or CK1 $\delta$  significantly decreases CHMP2B OE-induced hyperphosphorylation of enTDP-43. **(g and h)** The cell viability assay indicates that KD of CK1 $\alpha$  or CK1 $\delta$  markedly suppresses TDP-43 cytotoxicity and partially rescues CHMP2B OE-induced cell viability loss. **(i)** OE of CK1 $\alpha$  or CK1 $\delta$  diminishes the mitigating effect of siCHMP2B on TDP-43 cytotoxicity. **(j and k)** KD of TTBK1/2 reduces pTDP-43-HA levels in 293T cells. **(l and m)** KD of TTBK1/2 cannot suppress CHMP2B OE-induced hyperphosphorylation of enTDP-43. siCtrl, scrambled siRNA; siTTBK1/2, a mixture of siTTBK1 and siTTBK2. ud, undetected. Mean  $\pm$  SEM,  $n = 3–4$ . Two-tailed Student's  $t$  test (k) and one-way ANOVA with Tukey's HSD post-hoc test in all the rest; \*,  $P < 0.05$ ; \*\*,  $P < 0.01$ ; \*\*\*,  $P < 0.001$ . ns, not significant. Source data are available for this figure: SourceData F4.

We wondered how specific the function of CK1 was in mediating the modifying effect of CHMP2B on TDP-43 phosphorylation. The tau tubulin kinases 1 and 2 (TTBK1/2) were also reported to phosphorylate TDP-43 in previous studies (Liachko et al., 2014; Taylor et al., 2018), and we showed that KD of TTBK1/2 by siRNA (Fig. S4, c–e) was indeed able to lower TDP-43 phosphorylation levels (Fig. 4, j and k). However, unlike KD of CK1, down-regulation of TTBK1/2 failed to suppress CHMP2B OE-induced hyperphosphorylation of TDP-43 (Fig. 4, l and m). The results indicated that the kinases

TTBK1/2 do not underlie the function of CHMP2B in promoting TDP-43 phosphorylation and that CK1 acts as a rather specific molecular link between CHMP2B and TDP-43 phosphorylation.

#### Inhibition of CK1 alleviates CHMP2B-mediated TDP-43 hyperphosphorylation and cell death in neuroblastoma cells

CK1 inhibitors have been proposed as a drug candidate for treating TDP-43-associated ALS/FTD (Salado et al., 2014; Alquezar et al., 2016; Martínez-González et al., 2020). Here, we

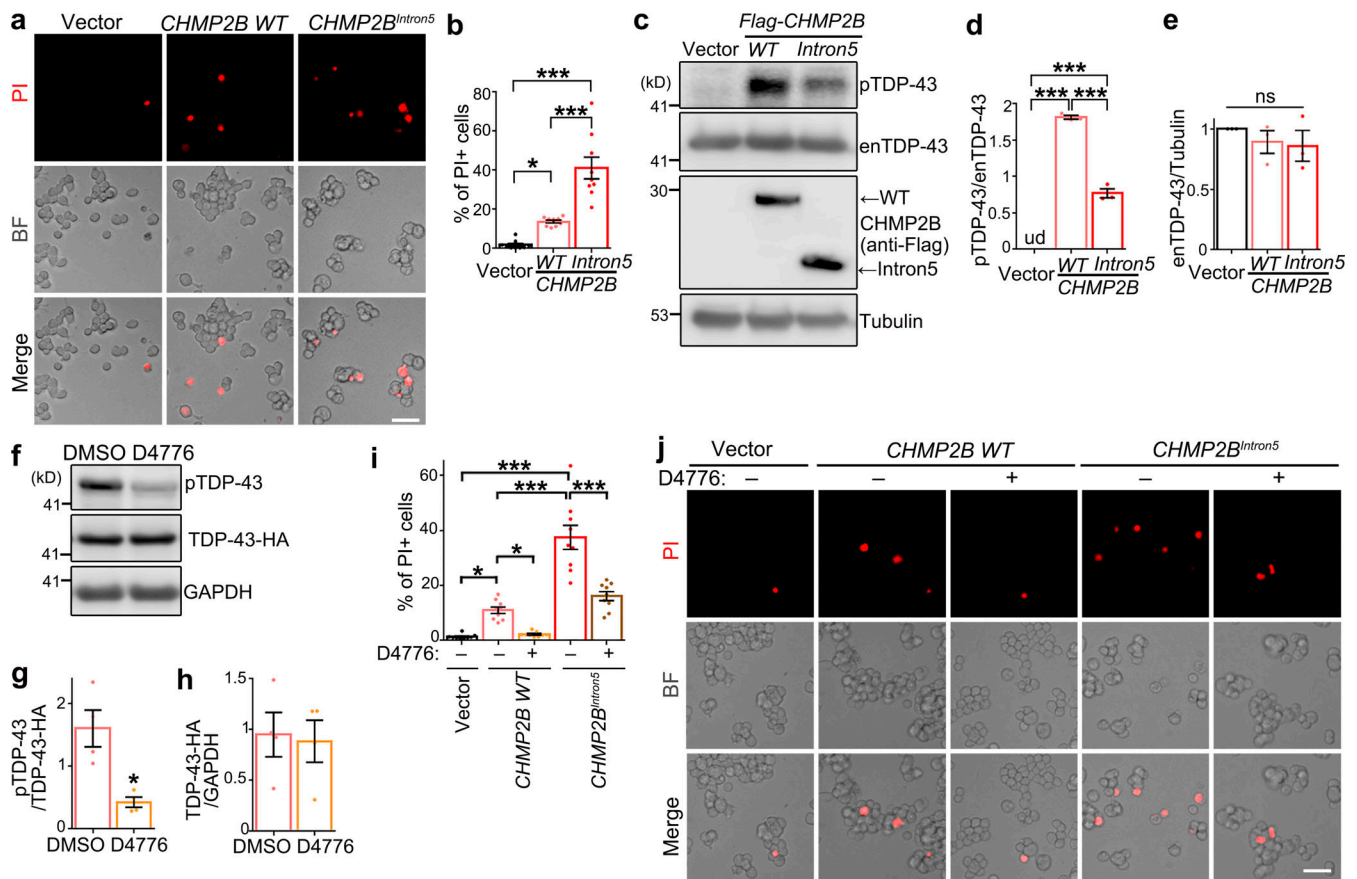


**Figure 5. CK1 inhibition diminishes CHMP2B-mediated cell death in neuroblastoma N2a cells. (a and b)** Representative PI staining images (a) and quantification (b) of the cell death of N2a cells transfected with WT *CHMP2B* or *CHMP2B<sup>Intron5</sup>*. **(c–e)** OE of WT *CHMP2B* or *CHMP2B<sup>Intron5</sup>* promotes hyperphosphorylation of endogenous TDP-43 (enTDP-43) in N2a cells, examined by Western blot (c) and quantified in (d and e). **(f–h)** The CK1 inhibitor D4776 (5 μM, 12 h) potently suppresses phosphorylation of TDP-43-HA in N2a cells. **(i and j)** Quantification (i) and representative PI staining images (j) show remarkable suppression of CHMP2B-mediated cell death by the CK1 inhibitor D4776 in N2a cells. Vehicle control, DMSO. BF, brightfield. Mean ± SEM, n = ~500 cells each group of pooled results from three independent repeats (b and i) and n = 3–4 (d, e, g, and h). One-way ANOVA with Tukey’s HSD post-hoc test (b, d, e, and i) and two-tailed Student’s t test (g and h); \*, P < 0.05; \*\*\*, P < 0.001. ns, not significant. Scale bars, 50 μm. Source data are available for this figure: SourceData F5.

explored the therapeutic potential of CK1 inhibition in CHMP2B-related neurodegeneration. First, we showed that OE of WT *CHMP2B* in murine neuroblastoma N2a cells caused significant cell death in the propidium iodide (PI) staining assay and OE of *CHMP2B<sup>Intron5</sup>* caused even more (Fig. 5, a and b). Consistent with the results in 293T cells (Fig. 2, d–f), they both promoted hyperphosphorylation of endogenous TDP-43, although OE of *CHMP2B<sup>Intron5</sup>* was markedly less effective than OE of WT *CHMP2B* (Fig. 5, c–e). Next, we treated N2a cells with a commonly available CK1 inhibitor D4776 (Rena et al., 2004), which significantly decreased TDP-43 phosphorylation levels and did not alter its protein levels (Fig. 5, f–h). We showed that inhibition of CK1 by D4776 in N2a cells almost completely suppressed the cell death induced by OE of WT *CHMP2B* and partially suppressed the toxicity of *CHMP2B<sup>Intron5</sup>* (Fig. 5, i and j).

We noted that OE of *CHMP2B<sup>Intron5</sup>* induced significantly more cell death in N2a cells (Fig. 5, a and b) and more severe impediment of the autophagic flux in 293T cells (Fig. 3, l and m) than WT *CHMP2B*, whereas OE of WT *CHMP2B* caused a much greater increase of pTDP-43 levels than that of *CHMP2B<sup>Intron5</sup>*

(Fig. 2, d and e; and Fig. 5, c and d). As CHMP2B appeared to regulate autophagy and TDP-43 phosphorylation through different mechanisms, we speculated that the *CHMP2B<sup>Intron5</sup>* mutation might have dominant or hypermorphic activity in the autophagy–endolysosomal pathway but was a hypomorphic mutation with regard to the function in regulating TDP-43 phosphorylation. *CHMP2B<sup>Q206H</sup>* is a single-nucleotide (A→C) replacement causing a Glu-to-His mutation, which is associated with TDP-43 pathology in the spinal motor neurons and glia of ALS patients (Cox et al., 2010). We found that OE of *CHMP2B<sup>Q206H</sup>* increased TDP-43 phosphorylation (Fig. S5, a and b) and CK1 levels (Fig. S5, a, c, and d) to a similar extent as OE of WT *CHMP2B*. Thus, not all disease-linked *CHMP2B* mutations are associated with impaired function in promoting TDP-43 phosphorylation.

#### CHMP2B regulates CK1 abundance via the UPS-mediated protein turnover

Earlier in this study, we noticed that even a slight OE or KD of *CK1α* or *CK1δ* was sufficient to alter pTDP-43 levels (Fig. 4, a–d; and Fig. S4, a and b), suggesting that the protein abundance of

CK1 closely controlled TDP-43 phosphorylation levels in cells. It prompted us to test whether CHMP2B affected CK1 protein levels. Indeed, KD of *CHMP2B* reduced the protein levels of CK1 $\alpha$  and CK1 $\delta$  by ~50% (Fig. 6, a and b), whereas OE of *CHMP2B* increased their levels by approximately two- to threefold in 293T cells (Fig. 6, c and d). In contrast, KD of *Atg12* or *Atg17* did not alter the protein levels of CK1 $\alpha$  or CK1 $\delta$  (Fig. S3, f-h). Furthermore, we confirmed that lentiviral expression of the shRNA of *CHMP2B* significantly decreased the protein abundance of CK1 $\alpha$  and CK1 $\delta$  in primary mouse cortical neurons (Fig. 6, e and f). We then conducted a pulse-chase assay with cycloheximide to inhibit protein translation to examine the protein turnover rate. We found that KD of *CHMP2B* accelerated (Fig. 6, g and h), whereas OE of *CHMP2B* hindered (Fig. 6, i and j) the turnover of CK1 $\alpha$  and CK1 $\delta$ .

Next, we determined whether CK1 was degraded mainly through the UPS or the autophagy pathway. Blocking the proteasome-mediated degradation with MG132, but not the autophagy-lysosomal pathway with CQ, significantly slowed down the protein turnover of CK1 $\alpha$  and CK1 $\delta$  (Fig. 7, a-c). This was confirmed with another proteasome inhibitor bortezomib (Fig. 7, d-g). Together, these data indicated that the protein turnover of CK1 was mediated through the UPS, but not the autophagy pathway. This raised the possibility that CHMP2B might generally regulate the function of the proteasomal degradation machinery, thereby affecting the turnover of CK1 nonspecifically. To test this possibility, we conducted an in vitro proteasome activity assay and found that neither KD nor OE of *CHMP2B* significantly altered the proteasome function in cells (Fig. 7, h and i). These results indicate that manipulation of *CHMP2B* does not alter the overall proteasomal activity but rather modulates the turnover of CK1 specifically.

Protein ubiquitination plays an important role in regulating protein degradation, which can serve as a signal for protein disposal via the UPS pathway (Khaminets et al., 2016; Kirkin et al., 2009). Since CHMP2B did not appear to regulate the overall proteasomal activity in cells, we tested the possibility that CHMP2B might regulate the turnover of CK1 by modulating its ubiquitination levels. Our data showed that KD of *CHMP2B* increased (Fig. 8, a and b), whereas OE of *CHMP2B* reduced (Fig. 8, c and d), the ubiquitination levels of CK1 $\alpha$  and CK1 $\delta$  in 293T cells. The same effects were observed when testing KD or OE of *CHMP2B* in neural N2a cells (Fig. 8, e-h). Together, these data indicate that CHMP2B regulates the ubiquitination and turnover of CK1 via the UPS-dependent degradation pathway.

## Discussion

Rare mutations in *CHMP2B* are associated with ALS and FTD (Skibinski et al., 2005; Parkinson et al., 2006; Cox et al., 2010). Previous studies of *CHMP2B* mutations in cell and animal models point to a major deficit in the autophagy-endolysosomal pathway (Lee et al., 2007; van der Zee et al., 2008; Ghazi-Noori et al., 2012; Clayton et al., 2015; Vernay et al., 2016). In this study, we uncover a previously unknown function of CHMP2B in regulating TDP-43 phosphorylation. Interestingly, we show that genetic and pharmacological inhibition of autophagy does not alter

TDP-43 phosphorylation levels in flies or mammalian cells, suggesting that the function of CHMP2B in regulating TDP-43 phosphorylation is independent of its well-known function in the autophagy-endolysosomal pathway.

Another line of evidence supporting the independent, dual functions of CHMP2B in regulating autophagy and TDP-43 phosphorylation comes from the study of the disease-causing *CHMP2B* mutations. It is noted that OE of WT *CHMP2B* causes a much greater increase of TDP-43 phosphorylation than that of *CHMP2B<sup>Intron5</sup>*, while the latter causes a much stronger cytotoxicity and impediment of autophagy than WT *CHMP2B*. It appears that *CHMP2B<sup>Intron5</sup>* is hypermorphic or dominant mutation with regard to the function in autophagy but is a hypomorph in regulating TDP-43 phosphorylation (Fig. 9), which may underlie the lack of TDP-43 pathology in *CHMP2B<sup>Intron5</sup>*-linked FTD. In contrast, *CHMP2B<sup>Q206H</sup>*, an ALS-causing *CHMP2B* mutation that is associated with TDP-43 pathology and regarded as a LOF in autophagy (Cox et al., 2010), exhibits normal capability of increasing CK1 and TDP-43 phosphorylation levels. Thus, the functions of *CHMP2B* in regulating autophagy and TDP-43 phosphorylation can be disjointedly affected; a mutation in *CHMP2B* can make the allele a hypermorph or LOF for one function (autophagy) but a hypomorph or WT-like for the other (TDP-43 phosphorylation).

Although protein inclusions containing hyperphosphorylated TDP-43 are associated with ALS and FTD, there has been controversy whether phosphorylation of TDP-43 promotes toxicity or is only a consequence of TDP-43 deposition or even protective (Liachko et al., 2010; Li et al., 2011). In this study, we show that TDP-43 exhibits remarkable neurotoxicity and phosphorylation in fly neurons but is unassociated with significant insolubility, indicating that the phosphorylation levels and aggregation of TDP-43 are not always correlated. Furthermore, we demonstrate in mammalian 293T and N2a cells that decrease of TDP-43 phosphorylation levels by inhibition of CK1 with siRNA or small-molecule D4776 markedly suppresses TDP-43- and *CHMP2B*-induced cytotoxicity. Together, our data lend support to the view that TDP-43 phosphorylation is toxic and pathogenic and that inhibition of TDP-43 phosphorylation may be a druggable target for treating ALS and FTD.

Finally, we show that CHMP2B negatively regulates ubiquitination and the turnover of CK1 through the UPS-mediated pathway. It is not completely surprising that the ESCRT complex also functions in regulating protein ubiquitination. For example, CHMP5, another component of the ESCRT-III complex, was shown to interact with the deubiquitinase USP8 and regulate protein ubiquitination in immune cells (Adoro et al., 2017; Son et al., 2019). It will be interesting to investigate how CHMP2B regulates CK1 ubiquitination in the future. Nevertheless, our data indicate that CHMP2B suppresses ubiquitination and degradation of CK1, which regulates the protein abundance of CK1 and subsequently affects the phosphorylation levels of TDP-43. Collectively, our findings propose a model of the dual functions of CHMP2B in regulating autophagy and TDP-43 phosphorylation, which may act through different mechanisms and be distinctly affected by the same disease-causing mutation (Fig. 9).

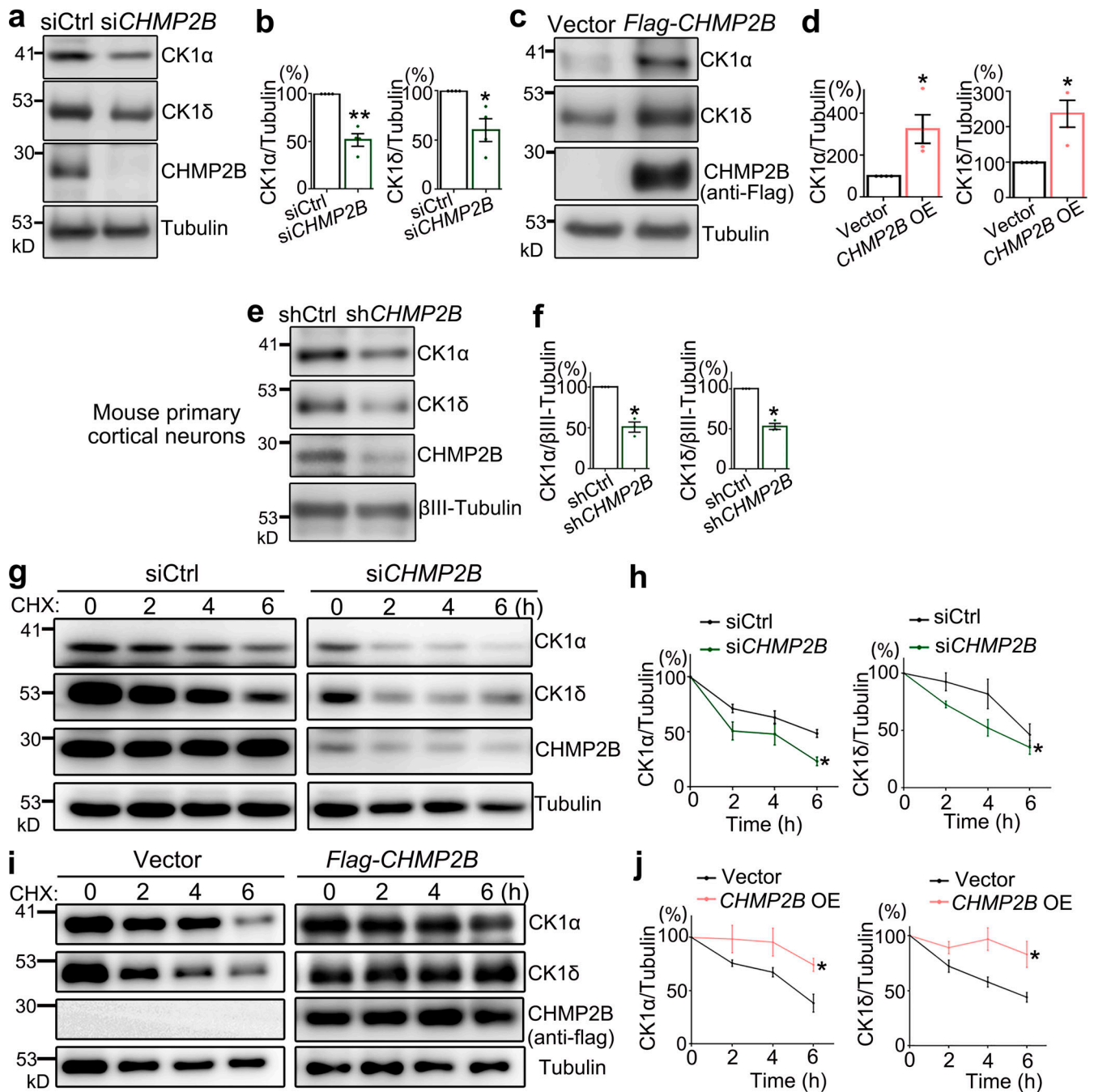


Figure 6. **CHMP2B controls the abundance of CK1α and CK1δ by regulating their protein turnover.** (a–d) Western blot analyses of the protein levels of CK1α and CK1δ with KD (a and b) or OE (c and d) of *CHMP2B* in 293T cells. (e and f) Lentiviral shRNA KD of *CHMP2B* decreases CK1α and CK1δ levels in mouse primary cortical neurons. (g–j) The pulse-chase assay to examine the protein turnover rates of CK1α and CK1δ with KD (g and h) or OE (i and j) of *CHMP2B*. All proteins are normalized to tubulin, and the relative level at 0 h is set to 100%. Mean ± SEM, n = 3–4. Two-sided Student's *t* test (b, d, and f) and two-way ANOVA with Bonferroni's post-hoc test (h and j); \*, P < 0.05; \*\*, P < 0.01. Source data are available for this figure: SourceData F6.

## Materials and methods

### *Drosophila* strains

The following strains were obtained from the Bloomington *Drosophila* Stock Center: UAS-*lacZ* (#8529, a control for UAS transgene expression), RNAi-*mCherry* (#35785, a control for short hairpin RNAi KD), RNAi-*luciferase* (#31603, a control for long hairpin RNAi KD), *elavGS* (#43642), RNAi-*CHMP2B* (#28531), UAS-RNAi-*Atg12* (#34675), and UAS-RNAi-*Atg17*

(#36918). The RNAi-*CHMP2B* (#38375) strain was obtained from the Tsinghua Fly Center. For the long hairpin RNAi line of *CHMP2B* (#28531), a copy of UAS-*Dcr2* was coexpressed to boost the KD efficiency (Ni et al., 2008).

The transgenic fly carrying the human *CHMP2B*<sup>Intron5</sup> mutation (UAS-Flag-*CHMP2B*<sup>Intron5</sup>) was generated by ΦC31 integrase-mediated, site-specific integration, and the attP landing site stock used was UAS-phi2b2a;VK5 (75B1). The

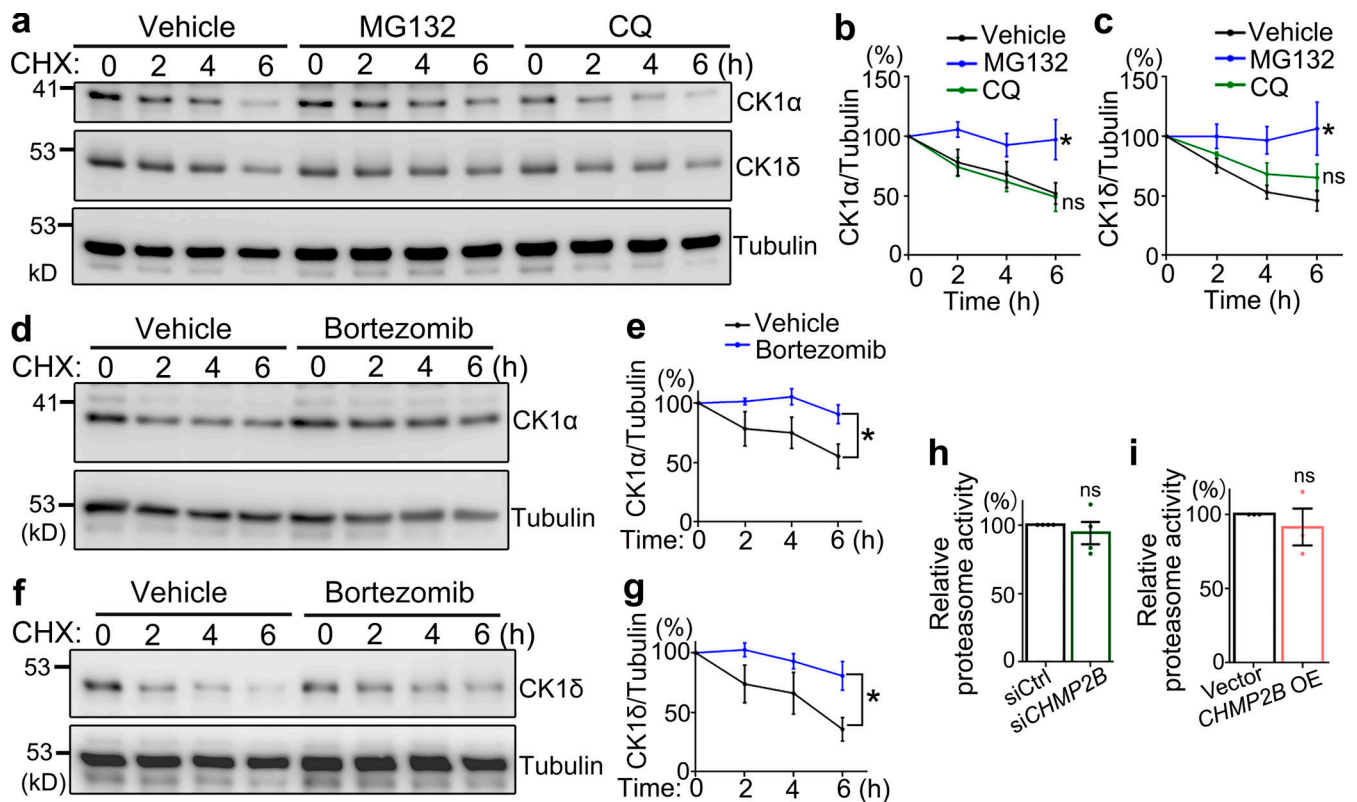


**Figure 7. CK1α and CK1δ are degraded through the proteasome-mediated pathway. (a–c)** The pulse-chase assay shows that inhibition of the proteasome activity by MG132 (10 μM), but not the autophagy pathway by CQ (10 μM), significantly delays the protein turnover of CK1α and CK1δ. **(d–g)** Inhibition of the proteasome function by bortezomib (10 μM) also suppresses the turnover of CK1α and CK1δ. CHX, cycloheximide. Vehicle control, DMSO. All proteins are normalized to tubulin and the relative levels at 0 h of each group are set to 100%. **(h and i)** The effects of KD (h) or OE (i) of WT *CHMP2B* on the proteasome activity in 293T cells are assessed using an in vitro fluorogenic peptide cleavage assay. The relative proteolytic activities are shown as average percentages to the total fluorescence intensity of the control group at the end of the assay (set to 100%). Means ± SEM; n = 3–4. Two-way ANOVA with Bonferroni’s post-hoc test (b, c, e, and g) and two-tailed Student’s *t* test (h and i); \*, P < 0.05. ns, not significant. Source data are available for this figure: SourceData F7.

UAS-*hTDP-43* flies (Sun et al., 2018) and the UAS-*luciferase* fly (Cao et al., 2017) were similarly generated using the same landing site, and the latter was used as a control.

Flies tested in this study were raised on standard cornmeal media and maintained at 25°C and 60% relative humidity. For adult onset, neuronal expression of the UAS, or RNAi transgenes using the *elavGS* driver (Osterwalder et al., 2001), flies were raised on regular fly food supplemented with 80 μg/ml RU486 (Tokyo Chemical Industry; M8046).

### Fly eye degeneration, lifespan, and climbing assays

The severity of the eye degeneration was assessed by rough surface, swelling, and loss of pigment cells of the compound eyes. Each fly eye was single-blindly scored in a scale of 0 to 5, with 0 indicating no degeneration and 5 indicating full degeneration.

For the lifespan experiment, 20 flies per vial and 6–10 vials per group were tested. Flies were transferred to fresh fly food every 3 d, and the number of dead flies of each vial was recorded. Flies lost before natural death through escape or accidental death were excluded from the final analysis. The median lifespan was calculated as the mean of the medians of each vial belonging to the same group, whereas the “50% survival” shown on the

survival curves was derived from compilation of all vials of the group.

For the climbing assay, 20 flies were transferred into an empty polystyrene vial and gently tapped down to the bottom of the vial. The number of flies that climbed over a distance of 3 cm within 10 s was recorded. The test was repeated three times for each vial, and five to eight vials of each genotype were assessed.

### RNA extraction and real-time qPCR

For qPCR, total RNA was isolated from fly heads or cell culture using TRIzol (Invitrogen; 15596018) according to the manufacturer’s instruction. After DNase (Promega; M6101) treatment to remove genomic DNA, the reverse transcription reactions were performed using All-in-One cDNA Synthesis SuperMix kit (Bimake; B24403). The cDNA was then used for real-time qPCR using 2x SYBR Select Master Mix (Thermo Fisher; 4472908) with the QuantStudio 6 Flex Real-Time PCR system (Life Technologies). The mRNA levels of *actin* were used as an internal control to normalize the mRNA levels of genes of interest. The following qPCR primers were used in this study: *dActin*-forward (F), 5′-GAGCGGGTTACTCTTTTCAC-3′; *dActin*-reverse (R), 5′-GCCATCTCTGCTCAAAGTC-3′; *dCHMP2B*-F: 5′-GAAAGAAAC

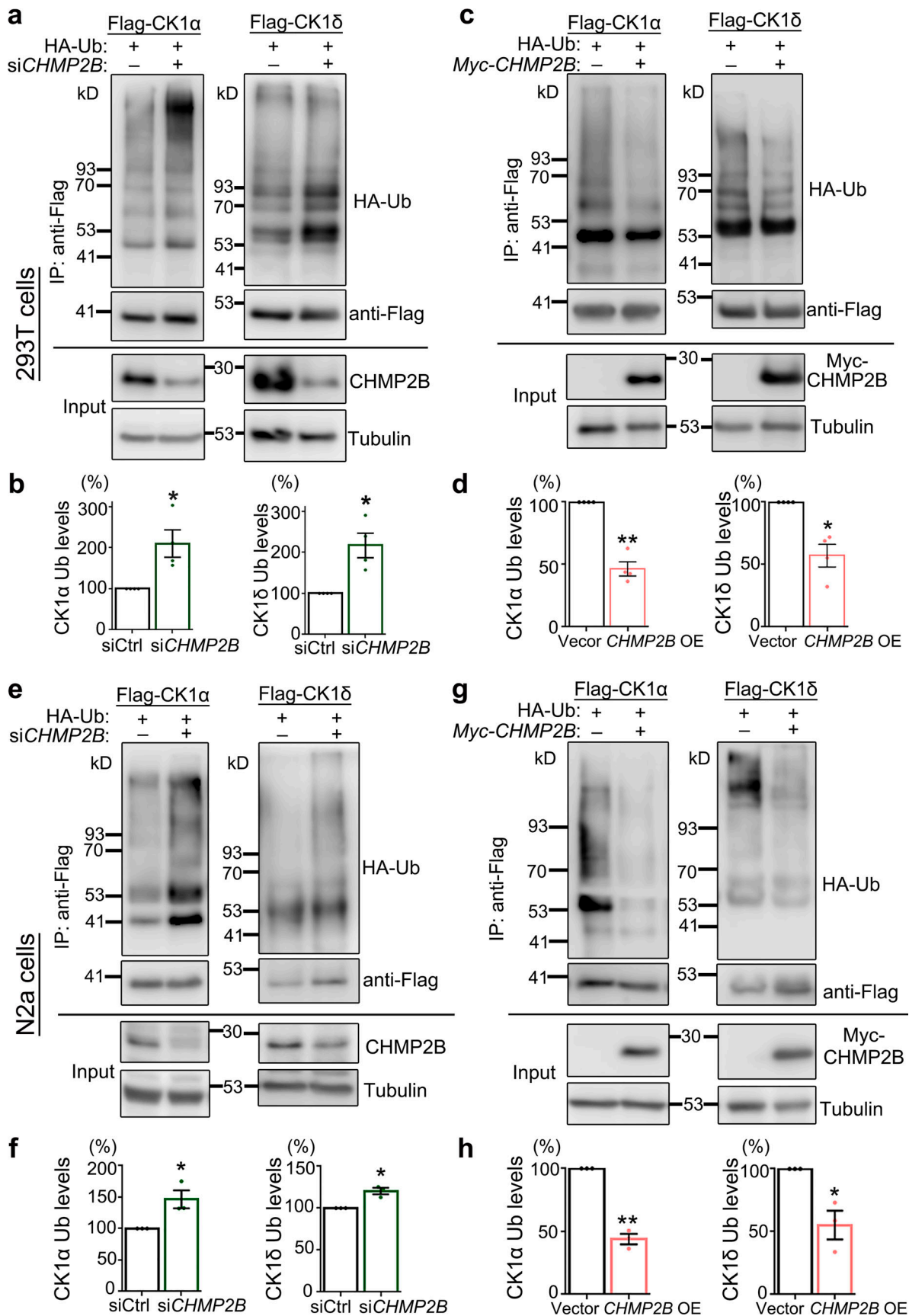


Figure 8. **CHMP2B modulates the ubiquitination levels of CK1.** (a–h) Representative Western blot images (a and c) and quantifications (b and d) of the impacts of KD (a and b) or OE (c and d) of CHMP2B on the ubiquitination levels of CK1α and CK1δ in 293T cells. The Flag-tagged CK1 proteins are

immunoprecipitated using an anti-Flag antibody, and the ubiquitination levels (HA-Ub) are examined by Western blotting. IP, immunoprecipitation. **(e-h)** The effects of KD (e and f) or OE (g and h) of *CHMP2B* on the ubiquitination levels of CK1 $\alpha$  and CK1 $\delta$  in N2a cells. Mean  $\pm$  SEM,  $n = 3-4$ . Two-tailed Student's  $t$  test; \*,  $P < 0.05$ ; \*\*,  $P < 0.01$ . Source data are available for this figure: SourceData F8.

CCACCGTGAAG-3'; dCHMP2B-R: 5'-TCCTCCTCCTCGATTTTCCT-3'.

#### Plasmids and siRNAs

The pCAG-*hTDP-43-HA* plasmid was described previously (Sun et al., 2018). In brief, DNA sequence encoding TDP-43 was amplified from a pcDNA3.1-TDP-43-myc plasmid (Jiang et al., 2013) by PCR using the primers containing the HA tag sequence. The PCR product was then subcloned into a pCAG vector (Chen et al., 2014) using the XhoI-EcoRI sites. The pcDNA3.1-HA-Ub plasmid was a kind gift from Z. Zhang (Chinese Academy of Sciences, Shanghai, China; Shi et al., 2019). To generate pCAG-*Flag-CHMP2B*, pCAG-*Flag-CK1 $\alpha$* , pCAG-*Flag-CK1 $\delta$* , pCAG-*Flag-TTBK1*, and pCAG-*Flag-TTBK2* plasmids, DNA fragments encoding human *CHMP2B*, *CK1 $\alpha$* , *CK1 $\delta$* , *TTBK1*, and *TTBK2* were amplified from pCMV3-*Flag-CHMP2B* (Sino Biological; #HG14596-NF) or cDNA from 293T or SH-SY5Y cells by PCR using the primers

containing the Flag tag sequence. The PCR products were then subcloned into a pCAG vector (Chen et al., 2014) using the XhoI-EcoRI sites. The following PCR primers were used: Flag-*CHMP2B-F*, 5'-CATCATTTTGGCAAAGAATTCCGCCACCATTGGATTACAAGGAT-3'; Flag-*CHMP2B-R*, 5'-GCTCCCCGGGGGTACCTCAGTTAATCTACTCTCTAA-3'; Flag-*CK1 $\alpha$ -F*, 5'-CATCATTTTGGCAAAGAATTCGCCACCATTGGATTACAAGGATGACGACGATAAGATGGCGAGTAGCAGC-3'; Flag-*CK1 $\alpha$ -R*, 5'-GCTCCCCGGGGGTACCTCGAGTTAGAAACCTTTCATGTTAC-3'; Flag-*CK1 $\delta$ -F*, 5'-CATCATTTTGGCAAAGAATTCGCCACCATTGGATTACAAGGATGACGACGATAAGATGGAGCTGAGAGTC-3'; Flag-*CK1 $\delta$ -R*, 5'-GCTCCCCGGGGGTACCTCGAGTCATCGGTGCACGAC-3'; Flag-*TTBK1-F*, 5'-CATCATTTTGGCAAAGAATTCCGCCACCATTGGATTACAAGGATGACGACGATAAGATGCAGTGCCTAGCGGCCG-3'; Flag-*TTBK1-R*, 5'-TGAGCTCCCCGGGGGTACCTCGAGTTATCTGGCCCCAGCCCGGC-3'; Flag-*TTBK2-F*, 5'-ATTTTGGCAAAGAATTCGCCACCATTGGATTACAAGGATGACGACGATAAGATGAGTG

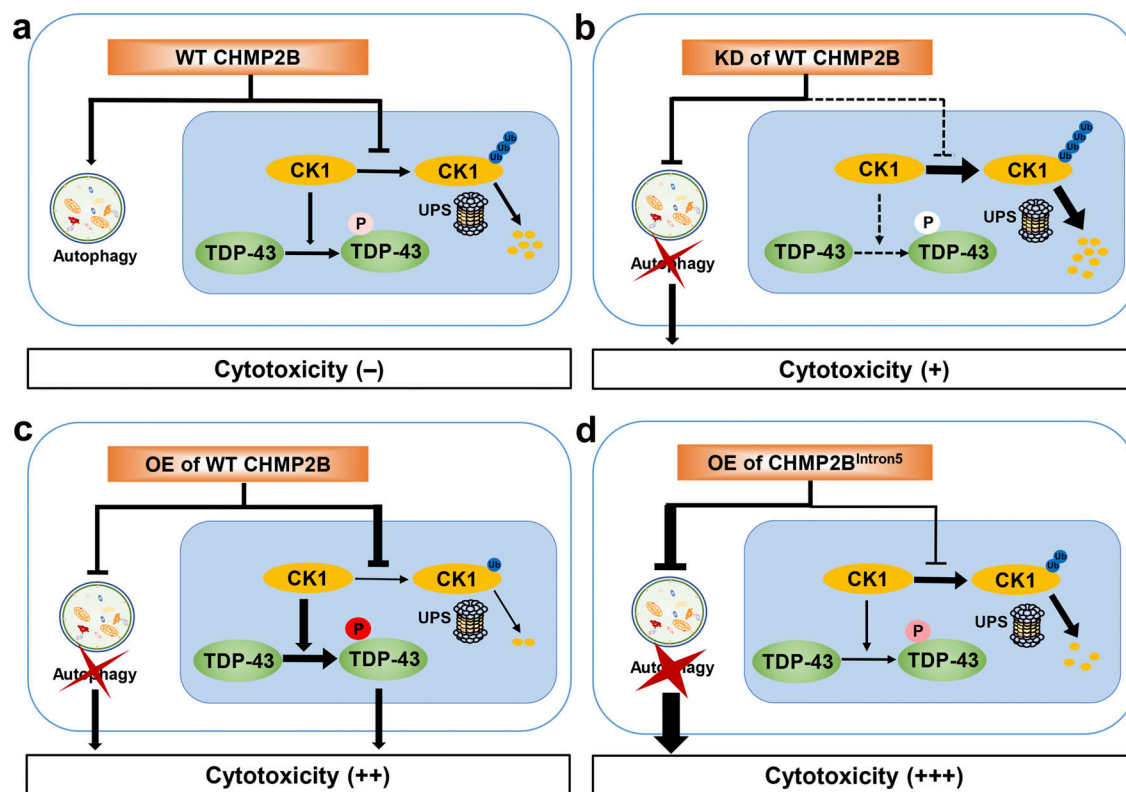


**Figure 9. A schematic model of the dual functions of CHMP2B in regulating autophagy and TDP-43 phosphorylation. (a)** A normal level and function of *CHMP2B* are required to maintain the autophagy function and suppress ubiquitination and protein turnover of the kinase CK1 that phosphorylates TDP-43. **(b)** KD of *CHMP2B* releases the suppression of CK1 ubiquitination, which promotes CK1 turnover, leading to decreased CK1 abundance and reduced TDP-43 phosphorylation levels. Meanwhile, down-regulation of *CHMP2B* causes autophagy impediment, leading to the cytotoxicity. **(c)** OE of *CHMP2B* also impairs the autophagy pathway. At the same time, it enhances the suppression of CK1 ubiquitination, which reduces CK1 degradation, increases CK1 levels, and promotes TDP-43 hyperphosphorylation. In this case, both impaired autophagy and increased TDP-43 phosphorylation contribute to the cytotoxicity. **(d)** The FTD-3-associated *CHMP2B<sup>Intron5</sup>* is a hypermorphic or dominant mutation that manifests strikingly more severe autophagy dysfunction and cytotoxicity than WT *CHMP2B* but is a hypomorph with regard to the function of *CHMP2B* in regulating TDP-43 phosphorylation. Together, *CHMP2B* plays the dual functions in regulating autophagy and TDP-43 phosphorylation, and the two functions may be executed independently through different mechanisms.

GGGGAGGAGAGC-3'; Flag-TTBK2-R, 5'-GAGCTCCCCGGGGT ACCTCGAGCTATCTGCTGAGTTACTGG-3'.

The pCAG-Flag-CHMP2B<sup>Intron5</sup>, pCAG-Flag-CHMP2B<sup>Q206H</sup>, and pBID-UASC-Flag-CHMP2B<sup>Intron5</sup> plasmids were generated by homologous recombination. Briefly, the DNA fragment of Flag-CHMP2B<sup>Intron5</sup> or Flag-CHMP2B<sup>Q206H</sup> was amplified by PCR and inserted into the cloning vector using ClonExpress MultiS One Step Cloning Kit (Vazyme; C113). The construct was then subcloned into the pCAG or pBID-UASC vector as above. The following PCR primers were used in this study: Flag-CHMP2B<sup>Intron5</sup>-F, 5'-CATCATTTTGGCAAAGAATTCGCCACCATG GATTACAAGGAT-3'; Flag-CHMP2B<sup>Intron5</sup>-R, 5'-GCTCCCCGGGGG TACCTCGAGTTACACCTTCCAGA-3'; Flag-CHMP2B<sup>Q206H</sup>-F, 5'-G AGATTGAACGGCACCTCAAGGCTTTAGGAGTAGATTAAGTTCG-3'; Flag-CHMP2B<sup>Q206H</sup>-R, 5'-CCTAAAGCCTTGAGGTGCCGTTCAATC TCTCATCTGAG-3'.

To generate the pLKO-shRNA-CHMP2B plasmid, the follow- ing sense and antisense oligos (GenePharma) of the mouse CHMP2B were annealed and then ligated with the digested pLKO.1 vector using the T4 DNA ligase (New England Biolabs; M0202S): sh-CHMP2B-F, 5'-CCGGCCCTTAAATAGCACGAACAT ACTCGAGTATGTTCTGCTATTTAAGGCTTTTGG-3'; sh-CHMP2B-R, 5'-AATTCAAAAAGCCTTAAATAGCACGAACATACTCGAGTA TGTTCTGCTATTTAAGGC-3'.

The negative control vector containing scrambled shRNA was obtained from Addgene (1864), and the sequence of the hairpin was 5'-CCTAAGGTTAAGTCGCCCTCGCTCGAGCGAGGGCGACTT AACCTTAGG-3'.

The siRNA oligonucleotides to CHMP2B, CK1 $\alpha$ , CK1 $\delta$ , TTBK1 and TTBK2 were purchased from GenePharma. A mixture of three independent siRNAs (1:1:1) was used for each targeted gene, and the sequences are as follows: siCtrl (scrambled siRNA), 5'-ACGUGACACGUUCGAGAA-3'; si-hCHMP2B#1, 5'-UUUAUU ACAUCAUCCACGG-3'; si-hCHMP2B#2, 5'-AGAUGCACAAGU UGUUUGG-3'; si-hCHMP2B#3, 5'-CAGAUGGUAAGCUUCGAGC-3'; si-CK1 $\alpha$ #1, 5'-UUCUACUGAUCUUCGUGC-3'; si-CK1 $\alpha$ #2, 5'-UAACUGGUUUAAUCCUGAG-3'; si-CK1 $\alpha$ #3, 5'-UUUCUGCUU UAACAUUGUC-3'; si-CK1 $\delta$ #1, 5'-CAUUUGGUCAGCAAGCAGC-3'; si-CK1 $\delta$ #2, 5'-UUGUCAAUCCAAGGUGC-3'; si-CK1 $\delta$ #3, 5'-AUUUCUGUCUCUUGGUGGC-3'; si-TTBK1#1, 5'-AAUGAACCU GCACACAUGG-3'; si-TTBK1#2, 5'-UUGCCCAGCCGCAAUGUGG-3'; si-TTBK1#3, 5'-AUGAUCACUGGUAGUCGG-3'; si-TTBK2#1, 5'-AAUUGGUAUUUGUCGAGC-3'; si-TTBK2#2, 5'-AUCAUU UCCAGUCUUCUCC-3'; si-TTBK2#3, 5'-AAGAGCUCAGGUUAA CAGC-3'; si-Atg12#1, 5'-GUUGCAGCUUCCUACUUA-3'; si- Atg12#2, 5'-CUGGCUGAAUACCUCAAA-3'; si-Atg12#3, 5'-GAG ACUAAGACUGUAUAAA-3'; si-Atg17#1, 5'-GGAGGACUGUUC AAAUUA-3'; si-Atg17#2, 5'-CGACCAUUUAUAGCAGAAU-3'; si-Atg17#3, 5'-CAGCUUGCAUUGGAAAUGU-3'; si-mCHMP2B#1, 5'-GGACGAUGUCAUAAAGGAA-3'; si-mCHMP2B#2, 5'-CCA CAGAAGACACUACAAA-3'; si-mCHMP2B#3, 5'-GGGAUUGAA AUCUCUGGAA-3'.

#### Cell culture and transfection

293T (American Type Culture Collection; CRL-11268) and N2a (American Type Culture Collection; CCL-131) cells were cultured in DMEM (Sigma-Aldrich; D0819) supplemented with 10% (vol/

vol) FBS (Biowest; S1710) and GlutaMAX (Invitrogen; 35050061) at 37°C in 5% CO<sub>2</sub>. Transient transfection of siRNA oligonu- cleotides or plasmids was performed using Lipofectamine RNAiMAX (Invitrogen; 13778075) in Opti-MEM (Invitrogen; 11058021) or the In Vitro DNA Transfection Reagent PolyJet (SigmaGen Laboratories; SL100688) in DMEM (Sigma-Aldrich; D0819). Cells were transfected with expression plasmids for 48 h or with siRNAs for 72 h before harvest.

#### Lentivirus production, primary neuron culture, and infection

To generate lentivirus for infecting primary neurons, 293T cells were cotransfected with pLKO-shRNA-CHMP2B, psPAX2, and pMD2.G with a ratio of 4:3:1 in DMEM (Sigma-Aldrich; D0819) using PolyJet (SigmaGen Laboratories; SL100688). The superna- tant of the cell culture was collected at 48 h after transfection and passed through a 0.45- $\mu$ m filter (Merck Millipore; SLHVR33RB). Fresh supernatant containing viral particles was used or stored at 4°C for less than 1 wk before infection of the primary neurons.

Primary cortical neurons were isolated from C57BL/6 mouse cortex at embryonic day 16 and cultured in serum-free Neurobasal medium (Invitrogen; 21103049) supplemented with 2% B27 (In- vitrogen; 17504044), GlutaMAX (Invitrogen; 35050061), and penicillin- streptomycin (Invitrogen; 10378016). At 5 d in vitro, neurons were infected with pLKO-shRNA-CHMP2B for 7 d before harvest.

#### Pharmacological experiments

For the pulse-chase assay, cycloheximide (Sigma-Aldrich; 01810) was added into the culture medium at a final concentration of 25 ng/ml. For inhibition of the proteasome or the autophagy- lysosome pathway, MG132 (Beyotime; S1748) or bortezomib (Selleck; S1013) was added at a final concentration of 10  $\mu$ M, Rapa (Selleck; S1039) was added at a final concentration of 100 nM, and CQ (Sigma-Aldrich; C6628) was added at a final con- centration of 10  $\mu$ M. For CK1 inhibition, D4776 (Selleck; S7642) was added at a final concentration of 5  $\mu$ M. The cells were treated with the above drugs for indicated durations and then harvested for the subsequent Western blotting.

#### Cell viability analysis and PI staining assay

293T cells were plated in 24-well plates at a density of 200,000 cells/ml and transfected with siRNAs or plasmids 12–24 h later. 6–8 h after transfection, the cells were seeded at 10,000 cells/ well into 96-well plates at a volume of 100  $\mu$ l/well. Cell viability was assessed by measuring the reduction of WST-8 (2-(2-me- thoxy-4-nitrophenyl)-3-(4-nitrophenyl)-5-(2, 4-disulphophenyl)- 2H-tetrazolium) into formazan using the CCK8 assay (Dojindo; CK04) by adding 10  $\mu$ l of CCK8 solution to the cells at specific time points. Thereafter, the cells were incubated for 2 h at 37°C before measurement of the OD values at 450 nm. Cell viability was quantified according to the manufacturer's instruction. PI staining to detect cell death was performed using the PI Staining Kit (Sangon Biotech; E607306) at 1  $\mu$ l/well of a 24-well plate at 37°C for 20 min according to the manufacturer's instruction.

#### Microscopic image acquisition

For PI staining, cells were imaged within the 24-well plate using a Leica DMi8 inverted live-cell microscopy system with a 20 $\times$ /

0.7 NA dry objective at room temperature. Images were captured using a 1.4 MP monochrome digital camera (Leica; DFC310FX) and processed using the Leica Application Suite X software. The images of the fly eyes were captured using an Olympus SZX16 stereomicroscope equipped with a 5 MP CCD color digital camera (Olympus; DP26-CU) at room temperature. The focus stacking was acquired and processed using Helicon Focus 6 and the cellSens Dimension software (Olympus). All images were assembled into figures using Adobe Photoshop CS6.

### Antibodies

The following antibodies were used in Western blotting, immunoprecipitation, and immunofluorescence assays: rabbit anti-phospho-TDP-43 (Ser409/Ser410; Sigma-Aldrich; SAB4200225), mouse anti-pTDP-43 (pSer409/Ser410; COSMO BIO CO, TIP-PTD-M01), mouse anti-FLAG (Sigma-Aldrich; F3165), rabbit anti-Flag (Proteintech; 20543-1-AP), mouse anti-HA (Proteintech; 66006-1), rabbit anti-HA (Cell Signaling Technology; 3724), rabbit anti-TDP-43 (Proteintech; 10782-2-AP), mouse anti-TDP-43 (Abcam; ab57105), mouse anti-P62/SQSTM1 (Proteintech; 66184-1-Ig), rabbit anti-LC3B (Abcam; ab48394), rabbit anti-ATG8A/GABARAP (Abcam; ab109364), rabbit anti-Ref(2)P (Abcam; ab178440), rabbit anti-CK1 $\alpha$  (Proteintech; 55192-1-AP), rabbit anti-CK1 $\delta$  (Proteintech; 14388-1-AP), mouse anti-GAPDH (Proteintech; 60004-1), rabbit anti-tubulin (MBL; PM054), mouse anti- $\beta$ -actin (Cell Signaling Technology; 3700), and rabbit anti- $\beta$ III-tubulin (Sigma-Aldrich; T2200). HRP-conjugated secondary antibodies included anti-mouse (Sigma-Aldrich; A4416) and anti-rabbit IgG (Sigma-Aldrich; A9169).

### Protein extraction and Western blotting

Fly heads or cultured cells were lysed in 2% SDS lysis buffer (100 mM Tris-HCl, pH 6.8, 2% SDS, 40% glycerol, 10%  $\beta$ -mercaptoethanol, and 0.04% bromophenol blue) or tissue extraction reagent I (50 mM Tris, pH 7.4, 250 mM NaCl, 5 mM EDTA, 2 mM Na<sub>2</sub>VO<sub>4</sub>, 1 mM NaF, 20 mM Na<sub>4</sub>P<sub>2</sub>O<sub>7</sub>, and 0.02% NaN<sub>3</sub>) containing protease (Roche; 5892791001) and phosphatase inhibitor cocktails (Roche; 04693132001).

All protein samples were boiled at 95°C for 5 min. Equal amounts of lysates were resolved by electrophoresis using a 10% Bis-Tris SDS-PAGE (Invitrogen; NP0303BOX). The 0.45- $\mu$ m Immobilon-P polyvinylidene fluoride transfer membrane for Western blotting (Merck Millipore; IPVH00010) were used, which were then probed with the primary and secondary antibodies listed above. Detection was performed using the High-sig ECL Western Blotting Substrate (Tanon; e168230). Images were captured using an Amersham Imager 600 (GE Healthcare) and the densitometry was measured using ImageQuant TL Software (GE Healthcare) and ImageJ. The contrast and brightness were optimized equally in Adobe Photoshop CS6. Tubulin, GAPDH, or  $\beta$ -actin was used as a loading control for normalization as indicated in the figures. The loading control is selected mainly according to the molecular weight of the proteins to be detected, the origin of each antibody, and the source of the protein samples.

### Immunoprecipitation

293T cells were lysed in an IP buffer (50 mM Tris-HCl, pH 7.4, 150 mM NaCl, 1% NP-40, 1 mM EDTA, and 5% glycerol)

containing protease inhibitor cocktails (Roche; 5892791001) and N-ethylmaleimide (Sigma-Aldrich; E3876). Following centrifugation at 15,000  $\times$  *g* for 15 min at 4°C, the supernatants were collected in new vials and incubated with mouse anti-Flag beads on a rotary shaker at 4°C overnight. The beads were then collected and eluted in the 2X SDS buffer for the subsequent Western blotting assay.

### In vitro proteasome activity assay

Proteasomal activity was measured using a proteasome activity assay kit (Abcam; ab107921). 293T cells were transfected with indicated plasmids for 48 h and siRNA for 72 h, followed by trypsin digestion and quantification. The cells were subsequently lysed in 90  $\mu$ l lysis buffer (0.5% NP-40 in PBS), and the lysates were centrifuged at 16,000  $\times$  *g* for 15 min at 4°C; then, the supernatants were collected in new vials. The proteasomal activity of the supernatants was determined by assaying the cleavage of a fluorogenic peptide substrate Suc-LLVY-AMC according to the manufacturer's instruction. The substrate peptides were incubated with the cell lysates at 37°C for 1 h, and the fluorescence intensity was measured at the end of the assay using a BioTek microplate reader (excitation/emission = 350/440 nm).

### Statistical analysis

Statistical significance in this study is determined by one-way ANOVA with Tukey's honestly significant difference (HSD) post-hoc test, two-way ANOVA with Bonferroni's post-hoc test, or unpaired, two-tailed Student's *t* test with equal variance (\*, *P* < 0.05; \*\*, *P* < 0.01; \*\*\*, *P* < 0.001) as indicated. Error bars represent the SEM. Data distribution was assumed to be normal, but this was not formally tested.

### Online supplemental material

Fig. S1 shows the effects of CHMP2B KD by two independent transgenic RNAi strains (#38375 and #28531) in flies. Fig. S2 demonstrates that OE of CHMP2B<sup>Intron5</sup> increases the phosphorylation levels but does not induce significant insolubility of hTDP-43 in flies. Fig. S3 indicates that down-regulation of *Atg12* or *Atg17* suppresses TDP-43-induced cytotoxicity but does not alter pTDP-43 and CK1 levels in 293T cells. Fig. S4 displays the dose-dependent effect of KD or OE of CK1 on the cell viability and confirms the KD efficiency of si-TTBK1/2 in 293T cells. Fig. S5 shows the effects of different ALS/FTD-associated CHMP2B mutations on TDP-43 phosphorylation and CK1 levels.

### Acknowledgments

We thank the Bloomington *Drosophila* Stock Center and Tsinghua Fly Center for providing the fly strains, J. Yuan for careful proofreading, Z. Zhang (Chinese Academy of Sciences) for the pcDNA3.1-HA-Ub plasmid, S. Zhang for technical support, and members of the Fang laboratory for helpful discussion.

This work is supported by the National Natural Science Foundation of China (grant 31970697), the Science and Technology Commission of Shanghai Municipality (grants 2019SHZDZX02, 20490712600, and 201409003300; to Y. Fang),

the National Natural Science Foundation of China (grant 82071372), Natural Science Foundation of Guangdong Province of China (grant 2021A1515011231), the Outstanding Scholar Program of Bioland Laboratory (Guangzhou Regenerative Medicine and Health Guangdong Laboratory; grant 2018GZ R110102002), the Science and Technology Program of Guangzhou (grant 202007030012), and the Guangdong Key Laboratory of Non-human Primate Research (grant 2020B121201006; to A. Li).

The authors declare no competing financial interests.

Author contributions: X. Sun, A. Li, and Y. Fang conceived the research; X. Deng, X. Sun, A. Li, and Y. Fang designed the experiments; X. Deng, X. Sun, W. Yue, Y. Duan, R. Hu, J. Ni, J. Cui, and Q. Wang performed the experiments; X. Deng, X. Sun, W. Yue, Y. Duan, R. Hu, and Y. Chen contributed important new reagents; X. Deng, X. Sun, W. Yue, K. Zhang, and Y. Fang analyzed the data and interpreted the results; X. Deng, X. Sun, and Y. Fang prepared the figures; and X. Deng, X. Sun, A. Li, and Y. Fang wrote the paper. All authors read and approved the final manuscript.

Submitted: 19 March 2021

Revised: 3 September 2021

Accepted: 4 October 2021

## References

- Adoro, S., K.H. Park, S.E. Bettigole, R. Lis, H.R. Shin, H. Seo, J.H. Kim, K.-P. Knobeloch, J.-H. Shim, and L.H. Glimcher. 2017. Post-translational control of T cell development by the ESCRT protein CHMP5. *Nat. Immunol.* 18:780–790. <https://doi.org/10.1038/ni.3764>
- Ahmad, S.T., S.T. Sweeney, J.A. Lee, N.T. Sweeney, and F.B. Gao. 2009. Genetic screen identifies serpin5 as a regulator of the toll pathway and CHMP2B toxicity associated with frontotemporal dementia. *Proc. Natl. Acad. Sci. USA.* 106:12168–12173. <https://doi.org/10.1073/pnas.0903134106>
- Alquezar, C., I.G. Salado, A. de la Encarnación, D.I. Pérez, F. Moreno, C. Gil, A.L. de Munain, A. Martínez, and Á. Martín-Requero. 2016. Targeting TDP-43 phosphorylation by Casein Kinase-1δ inhibitors: a novel strategy for the treatment of frontotemporal dementia. *Mol. Neurodegener.* 11: 36. <https://doi.org/10.1186/s13024-016-0102-7>
- Arai, T., I.R.A. Mackenzie, M. Hasegawa, T. Nonaka, K. Niizato, K. Tsuchiya, S. Iritani, M. Onaya, and H. Akiyama. 2009. Phosphorylated TDP-43 in Alzheimer's disease and dementia with Lewy bodies. *Acta Neuropathol.* 117:125–136. <https://doi.org/10.1007/s00401-008-0480-1>
- Bjørkøy, G., T. Lamark, A. Brech, H. Outzen, M. Perander, A. Overvatn, H. Stenmark, and T. Johansen. 2005. p62/SQSTM1 forms protein aggregates degraded by autophagy and has a protective effect on huntingtin-induced cell death. *J. Cell Biol.* 171:603–614. <https://doi.org/10.1083/jcb.200507002>
- Cao, X., H. Wang, Z. Wang, Q. Wang, S. Zhang, Y. Deng, and Y. Fang. 2017. In vivo imaging reveals mitophagy independence in the maintenance of axonal mitochondria during normal aging. *Aging Cell.* 16:1180–1190. <https://doi.org/10.1111/ace1.12654>
- Chang, X.L., M.S. Tan, L. Tan, and J.T. Yu. 2016. The Role of TDP-43 in Alzheimer's Disease. *Mol. Neurobiol.* 53:3349–3359. <https://doi.org/10.1007/s12035-015-9264-5>
- Chen, Y., Y. Wang, A. Ertürk, D. Kallop, Z. Jiang, R.M. Weimer, J. Kaminker, and M. Sheng. 2014. Activity-induced Nr4a1 regulates spine density and distribution pattern of excitatory synapses in pyramidal neurons. *Neuron.* 83:431–443. <https://doi.org/10.1016/j.neuron.2014.05.027>
- Chen-Plotkin, A.S., V.M. Lee, and J.Q. Trojanowski. 2010. TAR DNA-binding protein 43 in neurodegenerative disease. *Nat. Rev. Neurol.* 6:211–220. <https://doi.org/10.1038/nrneuro.2010.18>
- Cheong, J.K., and D.M. Virshup. 2011. Casein kinase 1: Complexity in the family. *Int. J. Biochem. Cell Biol.* 43:465–469. <https://doi.org/10.1016/j.biocel.2010.12.004>
- Choksi, D.K., B. Roy, S. Chatterjee, T. Yusuff, M.F. Bakhom, U. Sengupta, S. Ambegaokar, R. Kayed, and G.R. Jackson. 2014. TDP-43 Phosphorylation by casein kinase 1ε promotes oligomerization and enhances toxicity in vivo. *Hum. Mol. Genet.* 23:1025–1035. <https://doi.org/10.1093/hmg/ddt498>
- Clayton, E.L., S. Mizielinska, J.R. Edgar, T.T. Nielsen, S. Marshall, F.E. Norona, M. Robbins, H. Damiirji, I.E. Holm, P. Johannsen, et al. FReJA consortium. 2015. Frontotemporal dementia caused by CHMP2B mutation is characterised by neuronal lysosomal storage pathology. *Acta Neuropathol.* 130:511–523. <https://doi.org/10.1007/s00401-015-1475-3>
- Cohen, T.J., V.M. Lee, and J.Q. Trojanowski. 2011. TDP-43 functions and pathogenic mechanisms implicated in TDP-43 proteinopathies. *Trends Mol. Med.* 17:659–667. <https://doi.org/10.1016/j.molmed.2011.06.004>
- Cox, L.E., L. Ferraiuolo, E.F. Goodall, P.R. Heath, A. Higginbottom, H. Moritboys, H.C. Hollinger, J.A. Hartley, A. Brockington, C.E. Burness, et al. 2010. Mutations in CHMP2B in lower motor neuron predominant amyotrophic lateral sclerosis (ALS). *PLoS One.* 5:e9872. <https://doi.org/10.1371/journal.pone.0009872>
- Cozza, G., and L.A. Pinna. 2016. Casein kinases as potential therapeutic targets. *Expert Opin. Ther. Targets.* 20:319–340. <https://doi.org/10.1517/14728222.2016.1091883>
- Cruciat, C.-M. 2014. Casein kinase 1 and Wnt/β-catenin signaling. *Curr. Opin. Cell Biol.* 31:46–55. <https://doi.org/10.1016/j.ceb.2014.08.003>
- Filimonenko, M., S. Stuffers, C. Raiborg, A. Yamamoto, L. Malerød, E.M.C. Fisher, A. Isaacs, A. Brech, H. Stenmark, and A. Simonsen. 2007. Functional multivesicular bodies are required for autophagic clearance of protein aggregates associated with neurodegenerative disease. *J. Cell Biol.* 179:485–500. <https://doi.org/10.1083/jcb.200702115>
- Ghazi-Noori, S., K.E. Froud, S. Mizielinska, C. Powell, M. Smidak, M. Fernandez de Marco, C. O'Malley, M. Farmer, N. Parkinson, E.M.C. Fisher, et al. 2012. Progressive neuronal inclusion formation and axonal degeneration in CHMP2B mutant transgenic mice. *Brain.* 135:819–832. <https://doi.org/10.1093/brain/aws006>
- Hasegawa, M., T. Arai, T. Nonaka, F. Kametani, M. Yoshida, Y. Hashizume, T.G. Beach, E. Buratti, F. Baralle, M. Morita, et al. 2008. Phosphorylated TDP-43 in frontotemporal lobar degeneration and amyotrophic lateral sclerosis. *Ann. Neurol.* 64:60–70. <https://doi.org/10.1002/ana.21425>
- Henne, W.M., N.J. Buchkovich, and S.D. Emr. 2011. The ESCRT pathway. *Dev. Cell.* 21:77–91. <https://doi.org/10.1016/j.devcel.2011.05.015>
- Higashi, S., E. Iseki, R. Yamamoto, M. Minegishi, H. Hino, K. Fujisawa, T. Togo, O. Katsuse, H. Uchikado, Y. Furukawa, et al. 2007. Concurrence of TDP-43, tau and alpha-synuclein pathology in brains of Alzheimer's disease and dementia with Lewy bodies. *Brain Res.* 1184:284–294. <https://doi.org/10.1016/j.brainres.2007.09.048>
- Holm, I.E., E. Englund, I.R.A. Mackenzie, P. Johannsen, and A.M. Isaacs. 2007. A reassessment of the neuropathology of frontotemporal dementia linked to chromosome 3. *J. Neuropathol. Exp. Neurol.* 66:884–891. <https://doi.org/10.1097/nen.0b013e3181567f02>
- Isaacs, A.M., P. Johannsen, I. Holm, and J.E. Nielsen. FReJA consortium. 2011. Frontotemporal dementia caused by CHMP2B mutations. *Curr. Alzheimer Res.* 8:246–251. <https://doi.org/10.2174/156720511795563764>
- Jiang, J. 2017. CK1 in Developmental Signaling: Hedgehog and Wnt. *Top. Dev. Biol.* 123:303–329. <https://doi.org/10.1016/bs.ctdb.2016.09.002>
- Jiang, L.L., M.X. Che, J. Zhao, C.J. Zhou, M.Y. Xie, H.Y. Li, J.H. He, and H.Y. Hu. 2013. Structural transformation of the amyloidogenic core region of TDP-43 protein initiates its aggregation and cytoplasmic inclusion. *J. Biol. Chem.* 288:19614–19624. <https://doi.org/10.1074/jbc.M113.463828>
- Kabeya, Y., N. Mizushima, T. Ueno, A. Yamamoto, T. Kirisako, T. Noda, E. Kominami, Y. Ohsumi, and T. Yoshimori. 2000. LC3, a mammalian homologue of yeast Apg8p, is localized in autophagosomal membranes after processing. *EMBO J.* 19:5720–5728. <https://doi.org/10.1093/emboj/19.21.5720>
- Kametani, F., T. Nonaka, T. Suzuki, T. Arai, N. Dohmae, H. Akiyama, and M. Hasegawa. 2009. Identification of casein kinase-1 phosphorylation sites on TDP-43. *Biochem. Biophys. Res. Commun.* 382:405–409. <https://doi.org/10.1016/j.bbrc.2009.03.038>
- Khaminets, A., C. Behl, and I. Dikic. 2016. Ubiquitin-Dependent And Independent Signals In Selective Autophagy. *Trends Cell Biol.* 26:6–16. <https://doi.org/10.1016/j.tcb.2015.08.010>
- Kirkin, V., D.G. McEwan, I. Novak, and I. Dikic. 2009. A role for ubiquitin in selective autophagy. *Mol. Cell.* 34:259–269. <https://doi.org/10.1016/j.molcel.2009.04.026>
- Krasniak, C.S., and S.T. Ahmad. 2016. The role of CHMP2B<sup>Introm5</sup> in autophagy and frontotemporal dementia. *Brain Res.* 1649(Pt B):151–157. <https://doi.org/10.1016/j.brainres.2016.02.051>

- Lee, J.-A., and F.-B. Gao. 2009. Inhibition of autophagy induction delays neuronal cell loss caused by dysfunctional ESCRT-III in frontotemporal dementia. *J. Neurosci.* 29:8506–8511. <https://doi.org/10.1523/JNEUROSCI.0924-09.2009>
- Lee, J.-A., A. Beigneux, S.T. Ahmad, S.G. Young, and F.-B. Gao. 2007. ESCRT-III dysfunction causes autophagosome accumulation and neurodegeneration. *Curr. Biol.* 17:1561–1567. <https://doi.org/10.1016/j.cub.2007.07.029>
- Lee, J.-A., L. Liu, and F.-B. Gao. 2009. Autophagy defects contribute to neurodegeneration induced by dysfunctional ESCRT-III. *Autophagy.* 5: 1070–1072. <https://doi.org/10.4161/auto.5.7.9823>
- Lee, E.B., V.M. Lee, and J.Q. Trojanowski. 2011. Gains or losses: molecular mechanisms of TDP43-mediated neurodegeneration. *Nat. Rev. Neurosci.* 13:38–50. <https://doi.org/10.1038/nrn3121>
- Li, H.Y., P.A. Yeh, H.C. Chiu, C.Y. Tang, and B.P. Tu. 2011. Hyperphosphorylation as a defense mechanism to reduce TDP-43 aggregation. *PLoS One.* 6:e23075. <https://doi.org/10.1371/journal.pone.0023075>
- Liachko, N.F., C.R. Guthrie, and B.C. Kraemer. 2010. Phosphorylation promotes neurotoxicity in a *Caenorhabditis elegans* model of TDP-43 proteinopathy. *J. Neurosci.* 30:16208–16219. <https://doi.org/10.1523/JNEUROSCI.2911-10.2010>
- Liachko, N.F., P.J. McMillan, T.J. Strovass, E. Loomis, L. Greenup, J.R. Murrell, B. Ghetti, M.A. Raskind, T.J. Montine, T.D. Bird, et al. 2014. The tau tubulin kinases TTBK1/2 promote accumulation of pathological TDP-43. *PLoS Genet.* 10:e1004803. <https://doi.org/10.1371/journal.pgen.1004803>
- Ling, S.C., M. Polymenidou, and D.W. Cleveland. 2013. Converging mechanisms in ALS and FTD: disrupted RNA and protein homeostasis. *Neuron.* 79:416–438. <https://doi.org/10.1016/j.neuron.2013.07.033>
- Martínez-González, L., C. Rodríguez-Cueto, D. Cabezudo, F. Bartolomé, P. Andrés-Benito, I. Ferrer, C. Gil, Á. Martín-Requero, J. Fernández-Ruiz, A. Martínez, and E. de Lago. 2020. Motor neuron preservation and decrease of in vivo TDP-43 phosphorylation by protein CK-1δ kinase inhibitor treatment. *Sci. Rep.* 10:4449. <https://doi.org/10.1038/s41598-020-61265-y>
- Neumann, M., L.K. Kwong, D.M. Sampathu, J.Q. Trojanowski, and V.M.Y. Lee. 2007. TDP-43 proteinopathy in frontotemporal lobar degeneration and amyotrophic lateral sclerosis: protein misfolding diseases without amyloidosis. *Arch. Neurol.* 64:1388–1394. <https://doi.org/10.1001/archneur.64.10.1388>
- Neumann, M., L.K. Kwong, E.B. Lee, E. Kremmer, A. Flatley, Y. Xu, M.S. Forman, D. Troost, H.A. Kretschmar, J.Q. Trojanowski, and V.M. Lee. 2009. Phosphorylation of S409/410 of TDP-43 is a consistent feature in all sporadic and familial forms of TDP-43 proteinopathies. *Acta Neuropathol.* 117:137–149. <https://doi.org/10.1007/s00401-008-0477-9>
- Ni, J.Q., M. Markstein, R. Binari, B. Pfeiffer, L.P. Liu, C. Villalta, M. Booker, L. Perkins, and N. Perrimon. 2008. Vector and parameters for targeted transgenic RNA interference in *Drosophila melanogaster*. *Nat. Methods.* 5:49–51. <https://doi.org/10.1038/nmeth1146>
- Nonaka, T., G. Suzuki, Y. Tanaka, F. Kametani, S. Hirai, H. Okado, T. Miyashita, M. Saito, H. Akiyama, H. Masai, and M. Hasegawa. 2016. Phosphorylation of TAR DNA-binding Protein of 43 kDa (TDP-43) by Truncated Casein Kinase 1δ Triggers Mislocalization and Accumulation of TDP-43. *J. Biol. Chem.* 291:5473–5483. <https://doi.org/10.1074/jbc.M115.695379>
- Osterwalder, T., K.S. Yoon, B.H. White, and H. Keshishian. 2001. A conditional tissue-specific transgene expression system using inducible GAL4. *Proc. Natl. Acad. Sci. USA.* 98:12596–12601. <https://doi.org/10.1073/pnas.221303298>
- Parkinson, N., P.G. Ince, M.O. Smith, R. Highley, G. Skibinski, P.M. Andersen, K.E. Morrison, H.S. Pall, O. Hardiman, J. Collinge, et al. FReJA Consortium. 2006. ALS phenotypes with mutations in CHMP2B (charged multivesicular body protein 2B). *Neurology.* 67:1074–1077. <https://doi.org/10.1212/01.wnl.0000231510.89311.8b>
- Perez, P., A. Dray, D. Moore, P. Dietze, G. Bammer, R. Jenkinson, C. Siokou, R. Green, S.L. Hudson, and L. Maher. 2012. SimAmph: an agent-based simulation model for exploring the use of psychostimulants and related harm amongst young Australians. *Int. J. Drug Policy.* 23:62–71. <https://doi.org/10.1016/j.drugpo.2011.05.017>
- Rena, G., J. Bain, M. Elliott, and P. Cohen. 2004. D4476, a cell-permeant inhibitor of CK1, suppresses the site-specific phosphorylation and nuclear exclusion of FOXO1a. *EMBO Rep.* 5:60–65. <https://doi.org/10.1038/sj.embor.7400048>
- Salado, I.G., M. Redondo, M.L. Bello, C. Perez, N.F. Liachko, B.C. Kraemer, L. Miguel, M. Lecourtois, C. Gil, A. Martinez, and D.I. Perez. 2014. Protein kinase CK-1 inhibitors as new potential drugs for amyotrophic lateral sclerosis. *J. Med. Chem.* 57:2755–2772. <https://doi.org/10.1021/jm500065f>
- Shi, J., X. Hu, Y. Guo, L. Wang, J. Ji, J. Li, and Z.R. Zhang. 2019. A technique for delineating the unfolding requirements for substrate entry into retrotranslocons during endoplasmic reticulum-associated degradation. *J. Biol. Chem.* 294:20084–20096. <https://doi.org/10.1074/jbc.RA119.010019>
- Skibinski, G., N.J. Parkinson, J.M. Brown, L. Chakrabarti, S.L. Lloyd, H. Hummerich, J.E. Nielsen, J.R. Hodges, M.G. Spillantini, T. Thusgaard, et al. 2005. Mutations in the endosomal ESCRTIII-complex subunit CHMP2B in frontotemporal dementia. *Nat. Genet.* 37:806–808. <https://doi.org/10.1038/ng1609>
- Son, F., K. Umphred-Wilson, J.-H. Shim, and S. Adoro. 2019. Assessment of ESCRT Protein CHMP5 Activity on Client Protein Ubiquitination by Immunoprecipitation and Western Blotting. *Methods Mol. Biol.* 1998: 219–226. [https://doi.org/10.1007/978-1-4939-9492-2\\_16](https://doi.org/10.1007/978-1-4939-9492-2_16)
- Sun, X., Y. Duan, C. Qin, J.C. Li, G. Duan, X. Deng, J. Ni, X. Cao, K. Xiang, K. Tian, et al. 2018. Distinct multilevel misregulations of Parkin and PINK1 revealed in cell and animal models of TDP-43 proteinopathy. *Cell Death Dis.* 9:953. <https://doi.org/10.1038/s41419-018-1022-y>
- Tan, R.H., Y.D. Ke, L.M. Ittner, and G.M. Halliday. 2017. ALS/FTLD: experimental models and reality. *Acta Neuropathol.* 133:177–196. <https://doi.org/10.1007/s00401-016-1666-6>
- Taylor, L.M., P.J. McMillan, N.F. Liachko, T.J. Strovass, B. Ghetti, T.D. Bird, C.D. Keene, and B.C. Kraemer. 2018. Pathological phosphorylation of tau and TDP-43 by TTBK1 and TTBK2 drives neurodegeneration. *Mol. Neurodegener.* 13:7. <https://doi.org/10.1186/s13024-018-0237-9>
- Toyoshima, Y., and H. Takahashi. 2014. TDP-43 pathology in polyglutamine diseases: with reference to amyotrophic lateral sclerosis. *Neuropathology.* 34:77–82. <https://doi.org/10.1111/neup.12053>
- Urwin, H., S. Ghazi-Noori, J. Collinge, and A. Isaacs. 2009. The role of CHMP2B in frontotemporal dementia. *Biochem. Soc. Trans.* 37:208–212. <https://doi.org/10.1042/BST0370208>
- Urwin, H., A. Authier, J.E. Nielsen, D. Metcalf, C. Powell, K. Froud, D.S. Malcolm, I. Holm, P. Johannsen, J. Brown, et al. FReJA Consortium. 2010. Disruption of endocytic trafficking in frontotemporal dementia with CHMP2B mutations. *Hum. Mol. Genet.* 19:2228–2238. <https://doi.org/10.1093/hmg/ddq100>
- van der Zee, J., H. Urwin, S. Engelborghs, M. Bruyland, R. Vandenberghe, B. Dermaut, T. De Pooter, K. Peeters, P. Santens, P.P. De Deyn, et al. 2008. CHMP2B C-truncating mutations in frontotemporal lobar degeneration are associated with an aberrant endosomal phenotype in vitro. *Hum. Mol. Genet.* 17:313–322. <https://doi.org/10.1093/hmg/ddm309>
- Vernay, A., L. Therreau, B. Blot, V. Risson, S. Dirrig-Grosch, R. Waegaert, T. Lequeu, F. Sellal, L. Schaeffer, R. Sadoul, et al. 2016. A transgenic mouse expressing CHMP2B<sup>Bintron5</sup> mutant in neurons develops histological and behavioural features of amyotrophic lateral sclerosis and frontotemporal dementia. *Hum. Mol. Genet.* 25:3341–3360. <https://doi.org/10.1093/hmg/ddw182>
- Yamashita, T., S. Teramoto, and S. Kwak. 2016. Phosphorylated TDP-43 becomes resistant to cleavage by calpain: A regulatory role for phosphorylation in TDP-43 pathology of ALS/FTLD. *Neurosci. Res.* 107:63–69. <https://doi.org/10.1016/j.neures.2015.12.006>
- Zhang, Y.J., T.F. Gendron, Y.F. Xu, L.W. Ko, S.H. Yen, and L. Petrucelli. 2010. Phosphorylation regulates proteasomal-mediated degradation and solubility of TAR DNA binding protein-43 C-terminal fragments. *Mol. Neurodegener.* 5:33. <https://doi.org/10.1186/1750-1326-5-33>

Supplemental material

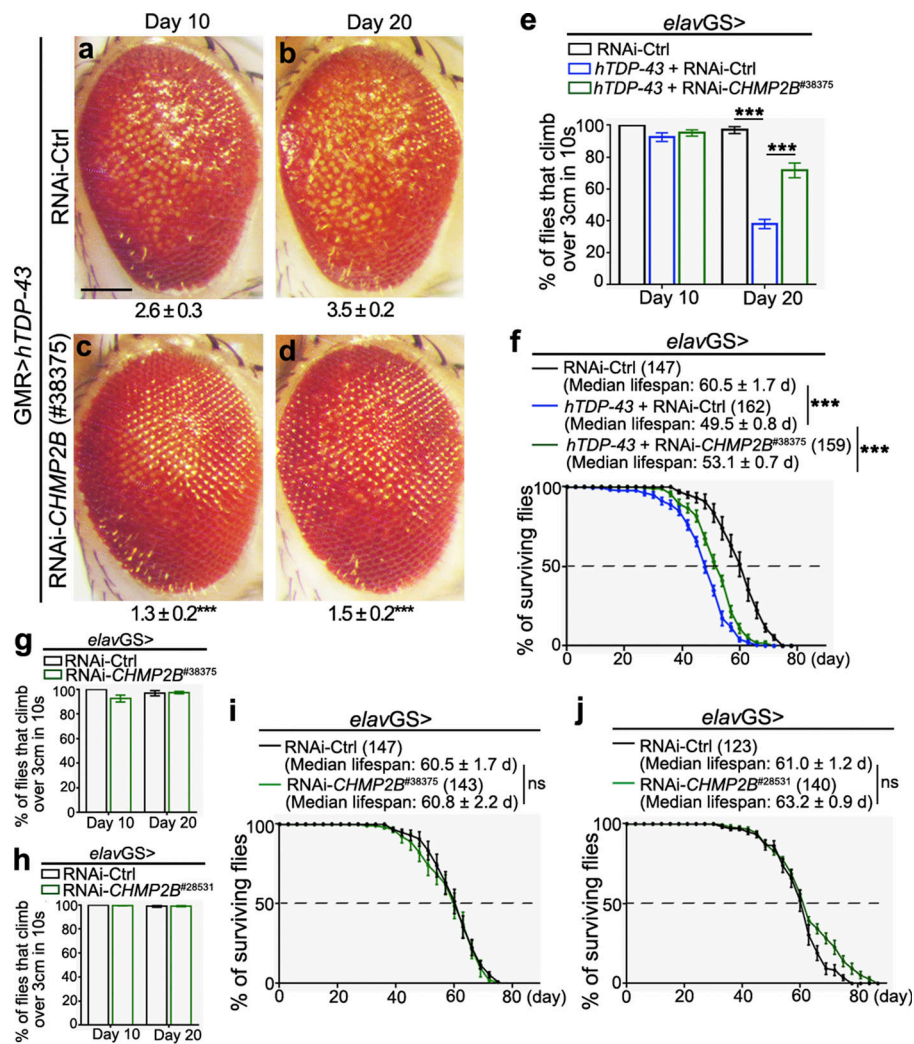


Figure S1. **KD of CHMP2B by two independent transgenic RNAi strains (#38375 and #28531) in flies.** (a-f) KD of CHMP2B by another RNAi fly line (#38375) also suppresses hTDP-43-induced eye degeneration (a-d), climbing deficits (e) and shortened lifespan (f). The degeneration score (mean ± SEM) and the statistical significance compared with the RNAi control (RNAi-*mCherry*) are indicated at the bottom of each group in (a-d). (g-j) KD of CHMP2B by the RNAi line #38375 (g and i) or #28531 (h and j) does not generally promote the climbing capability (g and h) or extend the lifespan (i and j) in flies. Data are shown as mean ± SEM; n = 10 eyes/group (a-d), n = 10 vials/group with ~20 flies/vial in (e, g, and h), n of flies and the median lifespan of each group are indicated (f, i, and j). Statistical significance is determined by two-tailed Student's *t* test in (a-d, g, and h), one-way ANOVA with Tukey's HSD post-hoc test (e), and two-way ANOVA with Bonferroni's post-hoc test (f, i, and j). \*\*\*, P < 0.001. ns, not significant. Scale bar, 100 μm.

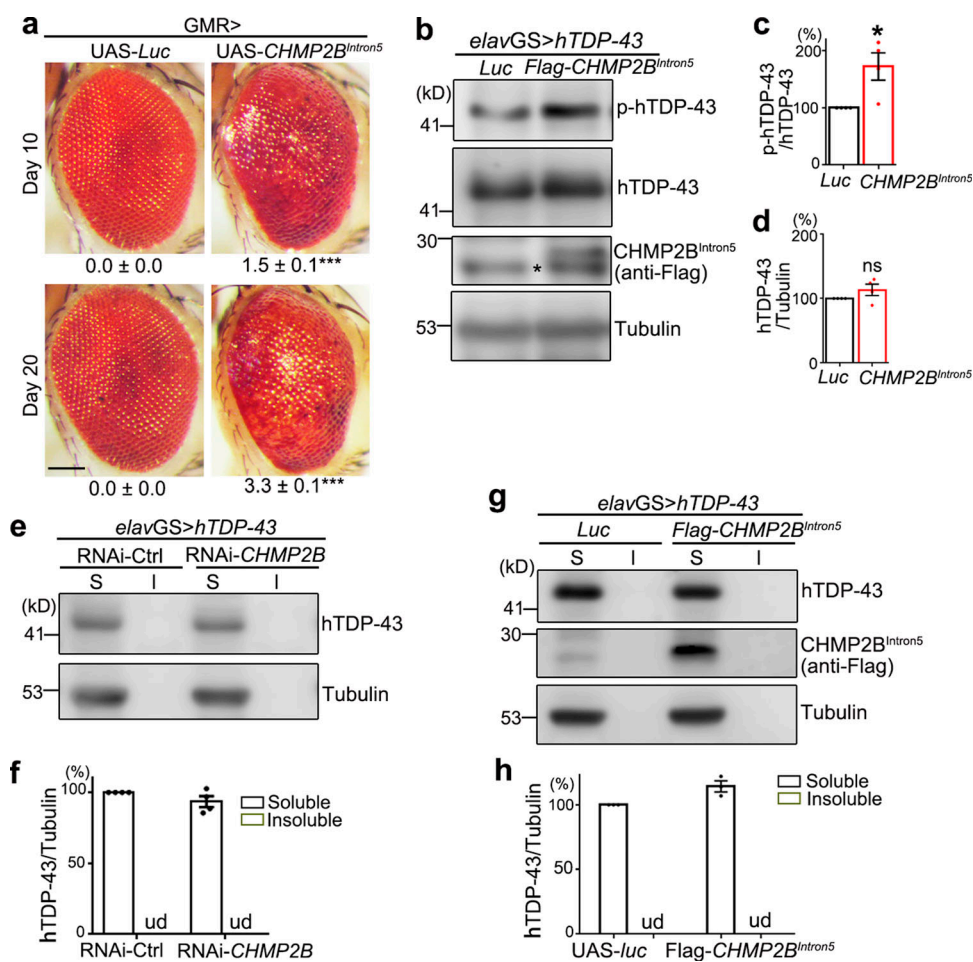


Figure S2. **OE of CHMP2B<sup>Intron5</sup> increases the phosphorylation levels but does not induce significant insolubility of hTDP-43 in flies.** (a) OE of the FTD-3-associated CHMP2B<sup>Intron5</sup> in flies (by GMR) causes the fly eye to degenerate. The degeneration score (mean ± SEM) and the statistical significance compared with the control flies (UAS-Luciferase, UAS-Luc) are indicated. (b-d) Western blot analysis (b) and quantifications of the phosphorylation (c) and total protein levels (d) of hTDP-43 in the heads of the transgenic flies overexpressing human CHMP2B<sup>Intron5</sup>. (e-h) KD of CHMP2B (e-f) or OE of CHMP2B<sup>Intron5</sup> (g and h) in fly heads does not alter the solubility of the transgenically expressed hTDP-43 protein. S, soluble fractions (the supernatants in RIPA); I, insoluble fractions (the pellets resuspended in 9 M urea). hTDP-43, human TDP-43; p-hTDP-43, phosphorylated hTDP-43. Asterisk indicates a nonspecific band close to the Flag-CHMP2B<sup>Intron5</sup> band in the anti-Flag blots of the fly samples. ud, undetected. All protein levels are normalized to tubulin in the soluble fraction. Mean ± SEM; n = ~10 eyes each group (a), n = 4 (c, d, and f), and n = 3 (h). Two-tailed Student's t test; \*, P < 0.05; \*\*\*, P < 0.001. ns, not significant. Scale bar, 100 μm. Source data are available for this figure: SourceData FS2.

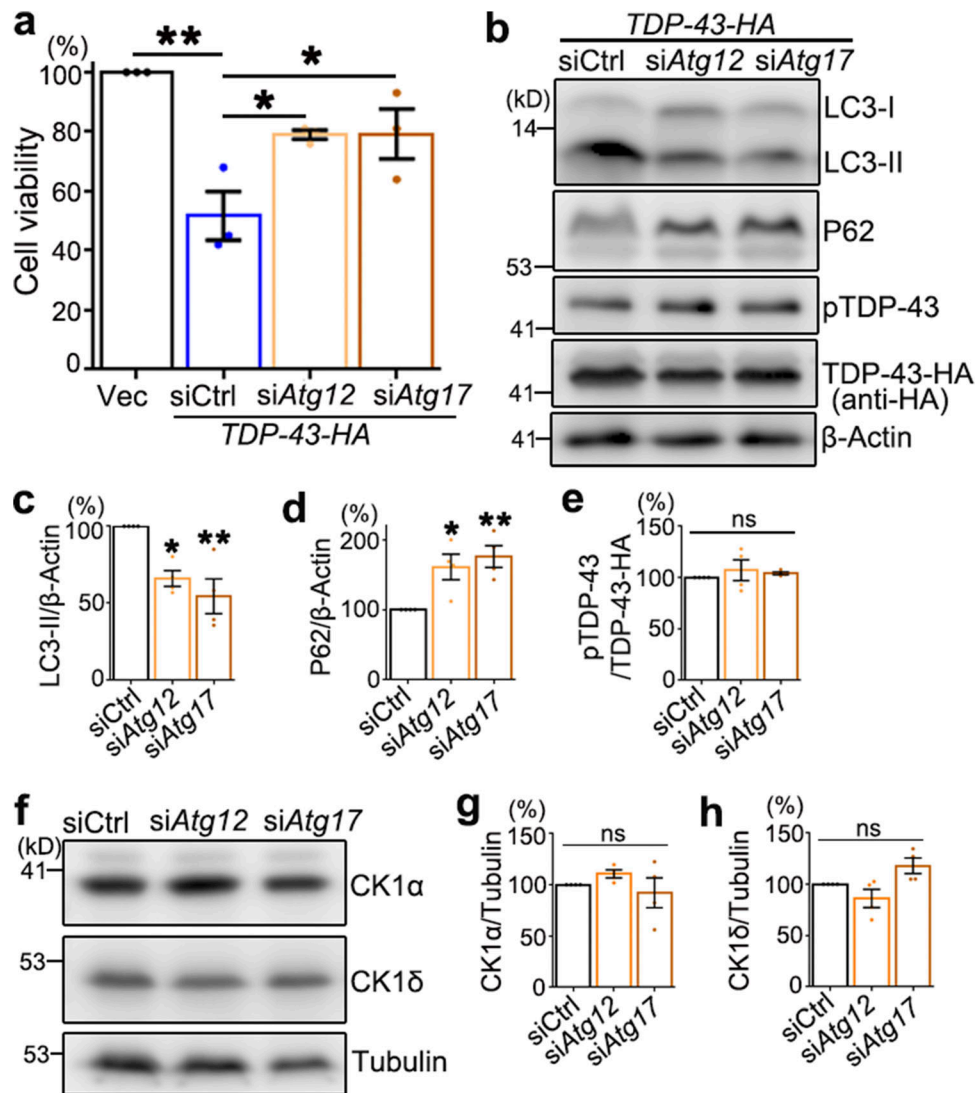


Figure S3. **Down-regulation of Atg12 or Atg17 suppresses TDP-43-induced cytotoxicity but does not alter pTDP-43 and CK1 levels in 293T cells.** (a) The viability of 293T cells transfected with the empty vector (Vec) or TDP-43-HA together with scrambled siRNA (siCtrl) or siRNA against Atg12 (siAtg12) or Atg17 (siAtg17) is assessed 72 h after transfection using the CCK8 assay. (b-e) Western blot analysis (b) and quantifications of LC3-II (c), P62 (d), and pTDP-43 (e) levels in 293T cells treated with siAtg12 or siAtg17. (f-h) Representative Western blot images (f) and quantifications of the CK1α (g) and CK1δ (h) normalized to tubulin. Mean ± SEM; n = 3-4. One-way ANOVA with Tukey's HSD post-hoc test; \*, P < 0.05; \*\*, P < 0.01. ns, not significant. Source data are available for this figure: SourceData FS3.

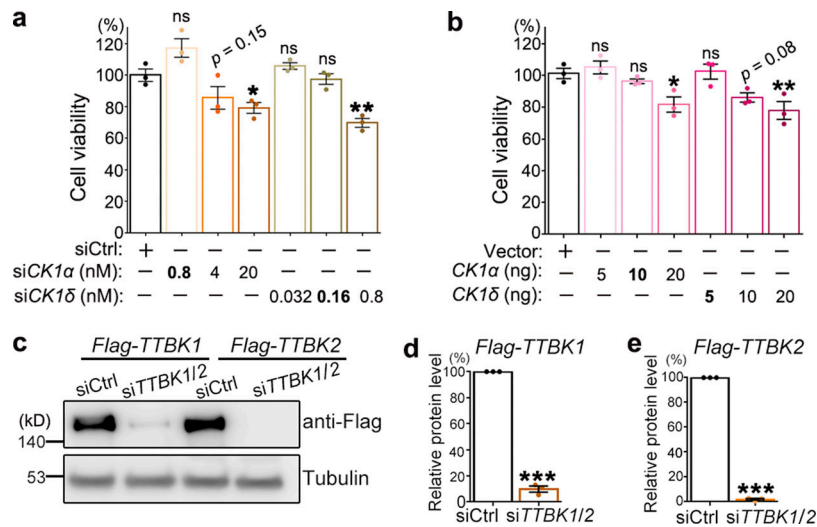


Figure S4. **Examination of the kinases CK1 and TTBK1/2 in 293T cells.** (a and b) The cell viability of 293T cells treated with siCK1 $\alpha$  or siCK1 $\delta$  (a) or transfected with Flag-CK1 $\alpha$  or Flag-CK1 $\delta$  (b) at indicated dosages is examined using the CCK8 assay. The statistical significance compared with the siCtrl (scrambled siRNA) or vector (empty vector) control is shown. KD of CK1 by transfection of 0.8 nM siCK1 $\alpha$  or 0.16 nM siCK1 $\delta$  and OE of CK1 by transfection of 10 ng CK1 $\alpha$  or 5 ng CK1 $\delta$  plasmids do not manifest significant loss of cell viability, which are used in the cell viability assays in Fig. 4, g-i. (c-e) Representative images (c) and quantifications (d and e) of the Western blot analysis confirming the down-regulation of TTBK1/2 by siTTBK1/2. Due to the lack of a good commercial anti-TTBK1/2 antibody, the transiently overexpressed Flag-TTBK1 and Flag-TTBK2 proteins are used as a readout to evaluate the KD efficiency of siTTBK1/2 (a mixture of siTTBK1 and siTTBK2 as used in Fig. 4, j-m). The siTTBK1/2 significantly reduces the protein levels of the overexpressed Flag-TTBK1 and Flag-TTBK2. Mean  $\pm$  SEM;  $n = 3$ . One-way ANOVA with Tukey's HSD post-hoc test (a and b) and two-tailed Student's  $t$  test in (d and e); \*,  $P < 0.05$ ; \*\*,  $P < 0.01$ ; \*\*\*,  $P < 0.001$ . ns, not significant. Source data are available for this figure: SourceData FS4.

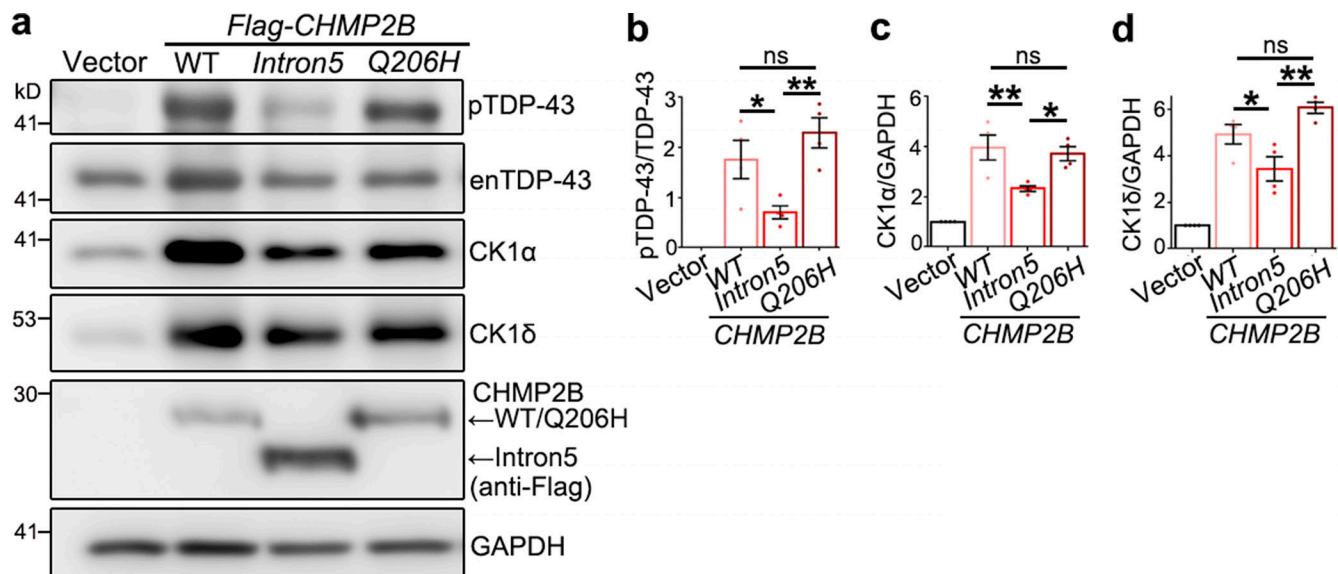


Figure S5. **The effects of different ALS/FTD-associated CHMP2B mutations on TDP-43 phosphorylation and CK1 levels.** (a-d) Representative Western blot images (a) and quantification of TDP-43 phosphorylation levels (b) and protein abundance of CK1 $\alpha$  (c) and CK1 $\delta$  (d) in 293T cells transfected with WT CHMP2B, CHMP2B<sup>Intron5</sup>, or CHMP2B<sup>Q206H</sup>. Cells transfected with the empty vector are used as a control. enTDP-43, endogenous TDP-43. Means  $\pm$  SEM;  $n = 4$ . One-way ANOVA with Tukey's HSD post-hoc test; \*,  $P < 0.05$ ; \*\*,  $P < 0.01$ . ns, not significant. Source data are available for this figure: SourceData FS5.